CHAPTER-4

RESULTS

CHAPTER- 4
RESULTS

4.1. Larval development parameters

Significant variations were observed in the developmental parameters of *S. ricini* larvae reared on three different food plants indoors, with an average room temperature of 25°C and a relative humidity of 75.18% (Table 4.1). Larval duration was found to be shortest in Sample C (19.87±0.26 days) followed by Sample T (20.63±0.34 days) and the longest in Sample P (24.67±0.36 days). However, the Sample C showed highest larval length (7.57±0.18 cm) and weight (6.92±0.21 g) followed by the Sample T (6.97±0.18 cm) and (5.71±0.26 g) respectively. Least larval length and weight were observed in Sample P (6.02±0.15 cm) and (4.33±0.21 g) respectively. Significant differences in percent of larval survivability were also observed in different treatment groups. The maximum survivability percent of larvae was recorded in Sample C (94.56±5.56 %) and lowest in Sample P (62.22±4.77 %) whereas Sample T showed moderate survivability percent (85.56±4.79 %). The silk gland weight of larvae was recorded highest in Sample C (1.42 ± 0.17 g) followed by Sample T (1.01±0.49 g) and lowest in Sample P (0.65±0.35 g). The length of the silk gland was also recorded highest in Sample C (54.67±3.79) followed by Sample T (51.33±5.31) and sample P (41.66±7.31) (Table 4.1).

Table 4.1. Growth parameters of *S. ricini* larvae reared on different food plants

Growth parameters	**Food plants**		
	Sample C (*S. ricini* on *R. communis*)	**Sample T (*S. ricini* on *M. esculenta*)**	**Sample P (*S. ricini* on *C. papaya*)**
Larval length (cm)	**7.57±0.18**	**6.97±0.18**	**6.02±0.15**
Larval weight (g)	**6.92±0.21**	**5.71±0.26**	**4.33±0.21**
Larval duration (days)	**19.87±0.26**	**20.63±0.34**	**24.67±0.36**
Survivability (%)	**94.56±4.56**	**85.56±4.79**	**62.22±4.77**
Weight of silk gland (g)	**1.42±0.17**	**1.01±0.49**	**0.65±0.35**
Length of silk gland (cm)	**54.67±3.79**	**51.33±5.31**	**41.66±7.31**

Data are presented as Mean ± SE x Z score @ 95% CI, Means with significant differences at ($P<0.05$)

4.2. Proximate analysis of sampled food plants leaves

Proximate analysis showed significant variation in the nutrient composition (moisture, crude fibre, fat, carbohydrate and crude protein contents) of three food plants *viz.* Castor, Tapioca and Papaya (Table 4.2). The results showed that the moisture content of papaya leaves was comparatively higher (6.11±0.49 g/100g) than castor (5.24±0.13 g/100g) and tapioca (5.69±0.12 g/100g). Additionally, the crude fibre content was higher in tapioca leaves (15.42±0.61 g/100g), followed by papaya (12.65±0.32 g/1100g) and castor leaves (8.40±0.27 g/100g).

Furthermore, the fat content was higher in papaya leaves (5.21±0.99 g/100g) followed by castor (2.16±0.42 g/100g) and tapioca leaves (1.12±0.55 g/100g). Similarly, the ash content was higher in papaya leaves (13.66±2.47 g/100g) followed by castor (10.52±0.28 g/100g) and tapioca (8.24±0.14g/100g). The crude protein content of castor leaves was recorded highest with (33.80±5.09 g/100g) followed by the protein content of tapioca (30.37±1.54 g/100g) and papaya leaves (28.61±2.01 g/100g). Likewise, the total carbohydrate content of the leaves was recorded highest in the castor leaves (40.37±2.59) followed by tapioca (39.16±1.55 g/100g) and papaya leaves (33.75±5.30 g/100g) (Table 4.2).

Table 4.2. Proximate analysis of food plants

Components	**Castor leaves (*R. communis*) (g/100g)**	**Tapioca leaves (*M. esculenta*) (g/100g)**	**Papaya leaves (*C. papaya*) (g/100g)**
Moisture	**5.24±0.13**	**5.69±0.12**	**6.11±0.49**
Crude fiber	**8.40±0.27**	**15.42±0.61**	**12.65±0.32**
Fat	**2.16±0.42**	**1.12±0.55**	**5.21±0.99**
Ash	**10.52±0.28**	**8.24±0.14**	**13.66±2.47**
Crude protein	**33.80±5.09**	**30.37±1.54**	**28.61±2.01**
Carbohydrate	**40.37±2.59**	**39.16±1.55**	**33.75±5.30**

Data are presented as Mean ± SE x Z score @ 95% CI, Means with significant differences at ($P<0.05$)

4.3. Gut digestive enzyme assay of *S. ricini* larvae

The results of all digestive enzyme activities were calculated using the standard curve used for each enzyme assay (Figure 4.1).

4.3.1. α-amylase activity

Significant variation in gut digestive enzyme activity was observed in the gut of *S. ricini* reared on three sampled food plants. The gut α-amylase showed highest activity in Sample C (4.57 ± 0.33 U/ml) followed by the Sample T (3.53± 0.05 U/ml) and Sample P with the lowest gut α-amylase activity (3.20 ± 0.07 U/ml) (Figure 4.2).

4.3.2. Cellulase activity

Gut cellulase activity was recorded highest in Sample C (0.58±0.01 U/ml) followed by Sample T (0.50±0.03 U/ml) and Sample P (0.22±0.02 U/ml). The variation in the enzyme activity was recorded significant at a level of ($P<0.05$) (Figure 4.2).

4.3.3. Proteinase activity

The gut proteinase activity assay revealed significant variations in the results in larvae fed with three types of food plants. The Sample P exhibited significantly higher gut proteinase activity (5.80± 1.46 U/ml) than other two samples. The Sample T showed moderate proteinase activity (2.46 ± 0.60 U/ml) whereas Sample C was recorded with lowest gut proteinase activity (2.41 ± 0.65 U/ml) (Figure 4.2).

4.3.4. Lipase activity

Significant difference in lipase activity was recorded in gut sample of Eri silkworm reared on castor, tapioca and papaya food plant leaves. The highest lipase activity was found in Sample C (0.56 ± 0.02 U/ml). In Sample T, the lipase activity was recorded as moderate (0.48 ± 0.13 U/ml) and the lowest gut lipase activity was observed in Sample P with activity (0.36 ± 0.02 U/ml) (Figure 4.2).

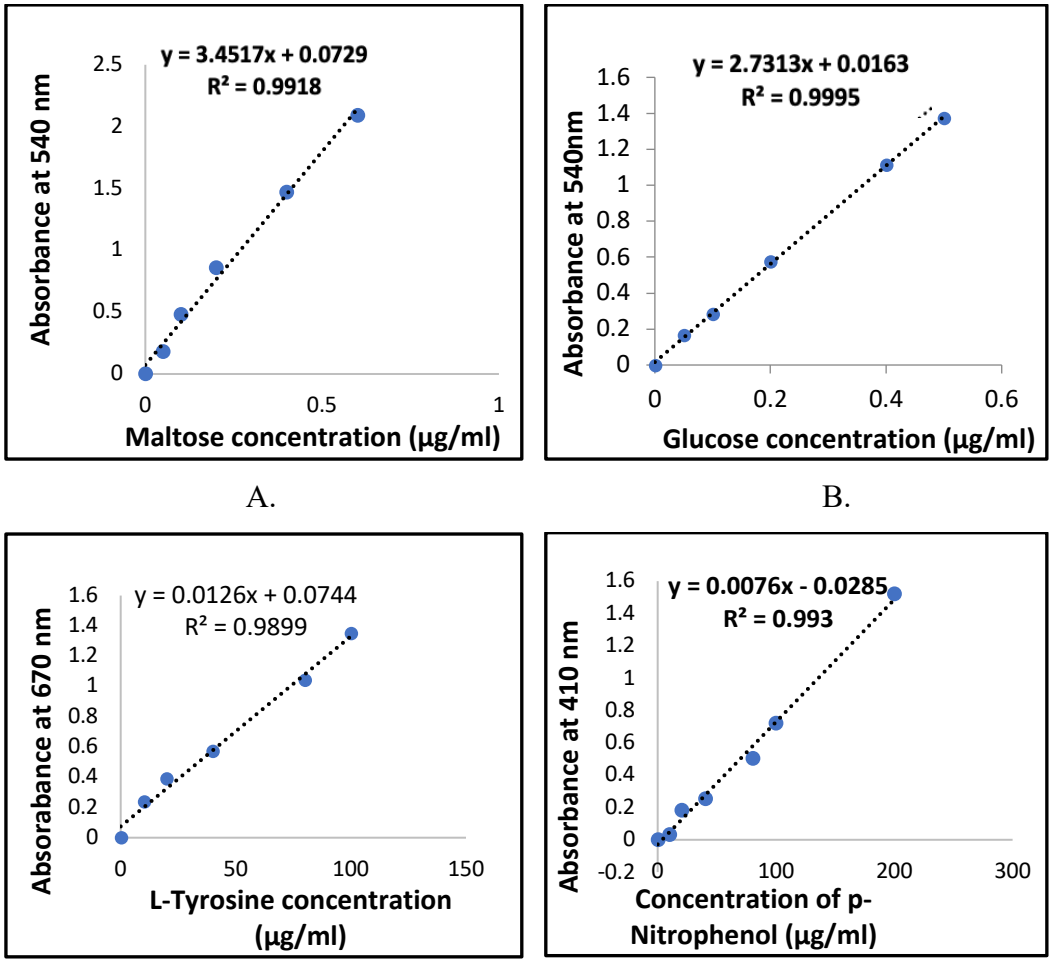

Figure 4.1. Standard curves for larval gut digestive enzyme assay: A. Maltose standard curve; B. D-glucose standard curve; C. L-Tyrosine standard curve; D. p-Nitrophenol standard curve

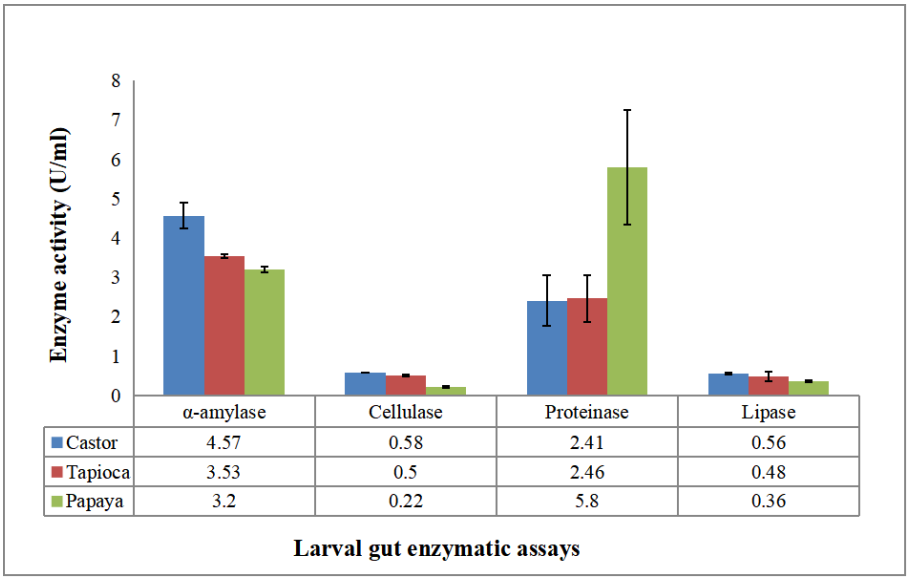

	α-amylase	Cellulase	Proteinase	Lipase
Castor	4.57	0.58	2.41	0.56
Tapioca	3.53	0.5	2.46	0.48
Papaya	3.2	0.22	5.8	0.36

Figure 4.2. Gut digestive enzyme activities of *S. ricini* larvae across three sampled food Plants

4.4. Study of the diversity of bacterial communities in the larval gut of silkworm *Samia ricini* feeding on different food plants using a culture independent method

4.4.1. Bacterial DNA isolation and quantification

The concentration of isolated DNA was quantified in Qubit Fluorimeter (V.3.0) yielding DNA concentrations of 120 ng/µl in Sample C, 22 ng/µl in Sample T and 4.4 ng/µl in Sample P (Table 4.3). Then, all the gel elutes were pooled separately for each sample to produce the minimal amount of starting DNA for further library preparation and sequencing process.

Table 4.3. DNA quantification result

Sl. No.	Sample Name	Qubit Concentration ng/µl	Total Gel Elute Conc. (ng)
1	Sample C	120	161.7
2	Sample T	22	136.5
3	Sample P	4.4	198.1

4.4.2. Quality Checking of PCR Amplicons and library preparation

The amplicons from all the three sampled showed bright bands at size 500bp (Figure 4.3) and taken for next process of library preparation in TapeStation library preparation kit. TapeStation profile estimated the modal fragment length of ~600bp in all the samples (Figure 4.4).

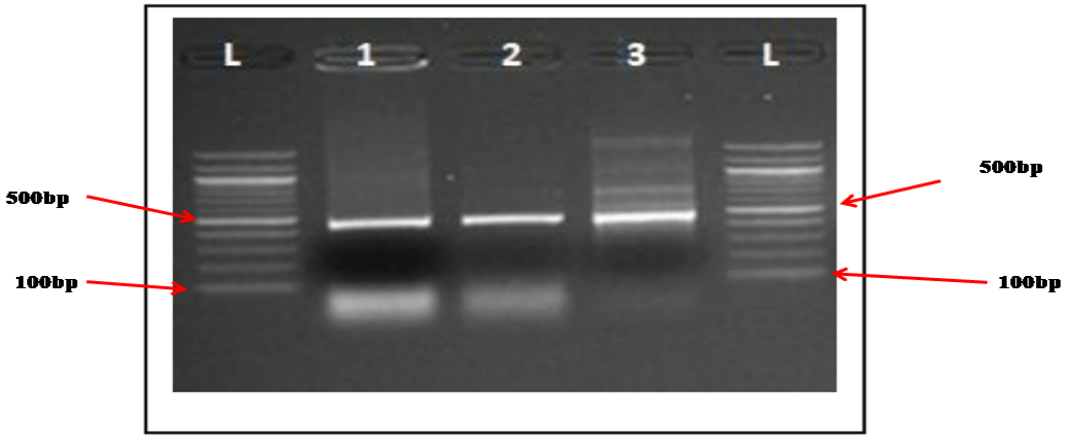

Figure 4.3. Gel electrophoresis profile of PCR amplicons: L= Ladder; 1= Sample C; 2= Sample T; 3= Sample P

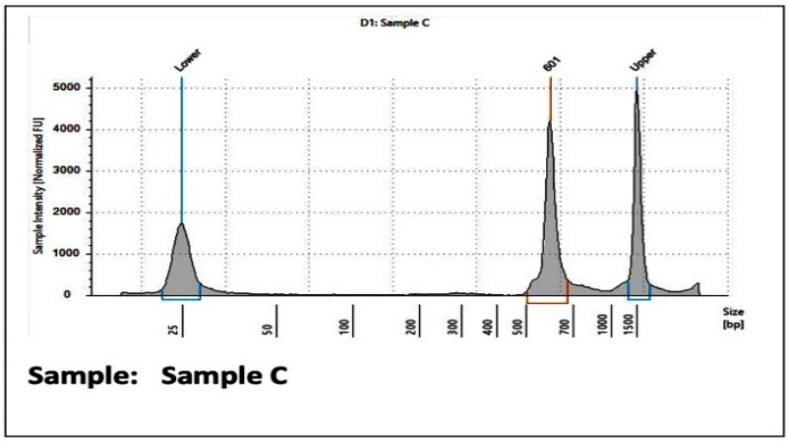

A.

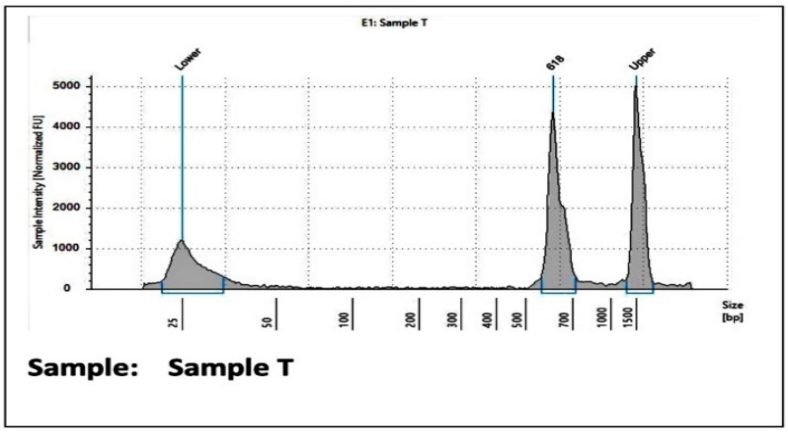

B.

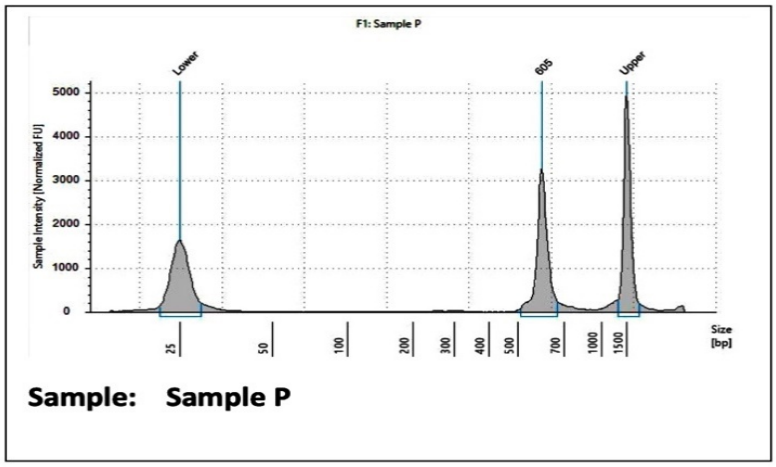

C.

Figure 4.4. Library preparation: TapeStation profile of A. sample C showing the expected size (601 bp) of the final library with a lower (25 bp) and upper (1500 bp) marker; B. TapeStation profile of sample T showing the expected size (618bp) of the final library with a lower (25 bp) and upper (1500 bp) marker; C. TapeStation profile of Sample P showing the expected size (605 bp) of the final library with a lower (25 bp) and upper (1500 bp) marker

4.4.3. Sequence quality checking report

I. Summary of raw reads

The Illumina 16S rRNA sequencing has generated pair end raw data with read orientations of R1 and R2 for each sample. Raw read quality check summary involved the assessment of base quality (Phred Score;Q), GC content, base composition and number of reads for both orientations in all the samples (Table 4.4).

Table 4.4. Sequencing data raw read summary

Sl. No.	Sample	Read orientation	Mean read quality (Phred score)	Number of reads	%GC	% Q < 10	%Q 10-20	%Q 20-30	%Q >30	Number of bases (MB)	Mean read length (bp)
1	Sample C	R1	36.30	64,500	54.84	0.00	3.87	2.08	94.05	16.12	250.00
		R2	35.49	64,500	55.09	0.00	6.17	3.12	90.71	16.12	250.00
2	Sample T	R1	36.03	79,716	54.39	0.00	4.36	2.54	93.10	19.93	250.00
		R2	35.53	79,716	54.26	0.00	5.93	3.25	90.82	19.93	250.00
3	Sample P	R1	36.27	427,103	55.64	0.00	3.79	2.10	94.10	106.78	250.00
		R2	35.50	427,103	55.83	0.00	5.96	3.16	90.89	106.78	250.00

II. Base quality score distribution

The base quality scores of each cycle for all samples indicate that across all samples, over 80% of the total reads possess Phred scores exceeding 30 (>Q30; error probability ≤0.001) (Table 4.5).

Table 4.5. Raw read summary with Phred quality score distribution (%)

Sl. No.	Sample Name	Q0-Q10	Q10-Q20	Q20-Q30	≥ Q30
1	Sample C	0.00	5.02	2.60	92.38
2	Sample T	0.00	5.15	2.89	91.96
3	Sample P	0.00	4.87	2.63	92.50

III. Base composition distribution

The compositions of nucleotides in the sequence read for each sample are shown in Table 4.6.

Table 4.6. Base composition distribution of the samples (%)

Sl. No.	Sample Name	A	C	G	T
1	Sample C	22.69	28.36	26.61	22.35
2	Sample T	23.20	27.84	26.48	22.47
4	Sample P	22.18	28.59	27.15	22.09

IV. GC distribution:

The distribution of average GC content among the sequenced reads from the samples typically falls within the 30-60% range. However, over 90% of the reads from all samples exhibit GC content clustered around 50%. The GC content distribution of all the samples has been depicted in the figures (Figure 4.5.1 to 4.5.3), with x-axis representing the average GC content in the sequence and y-axis indicating the percentage of sequence reads.

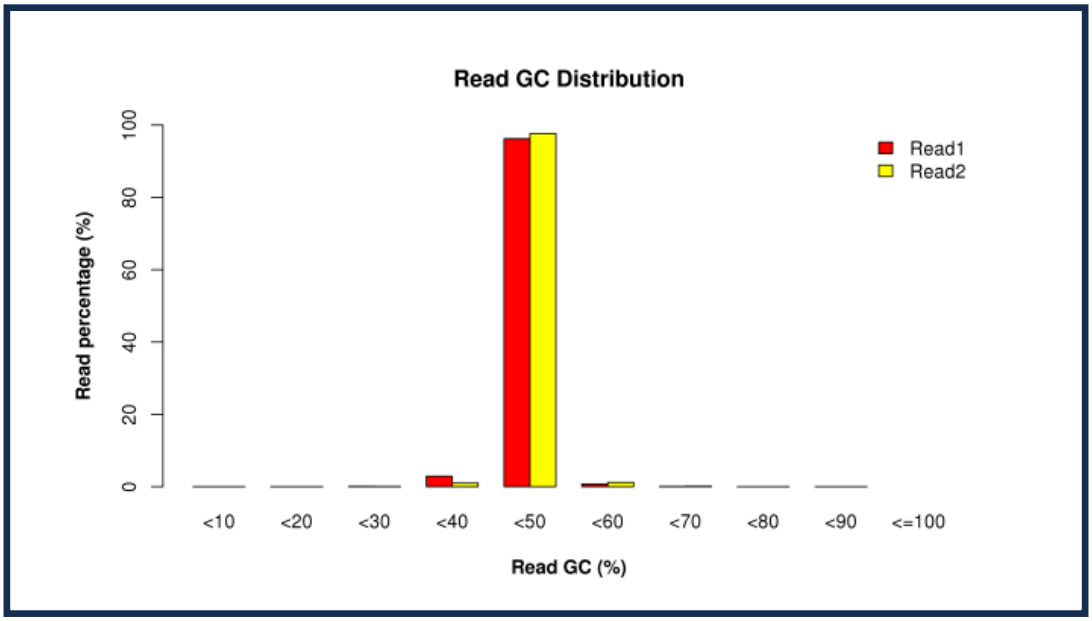

Figure 4.5.1. GC distribution plot of gut bacterial sequence reads from Sample C

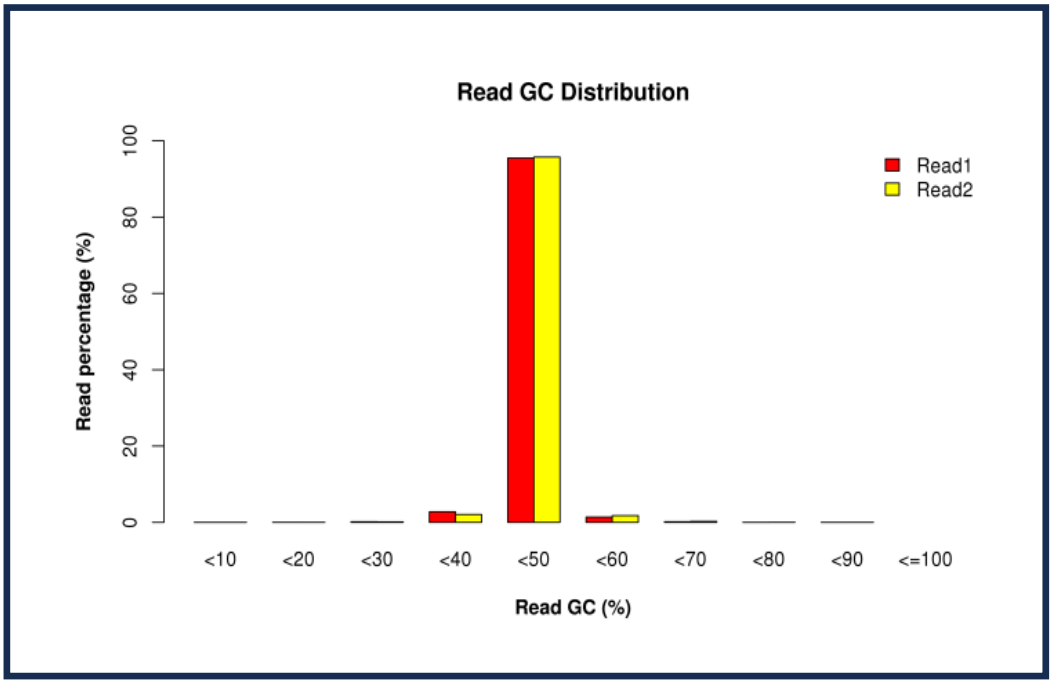

Figure 4.5.2. GC distribution plot of gut bacterial sequence reads from Sample T

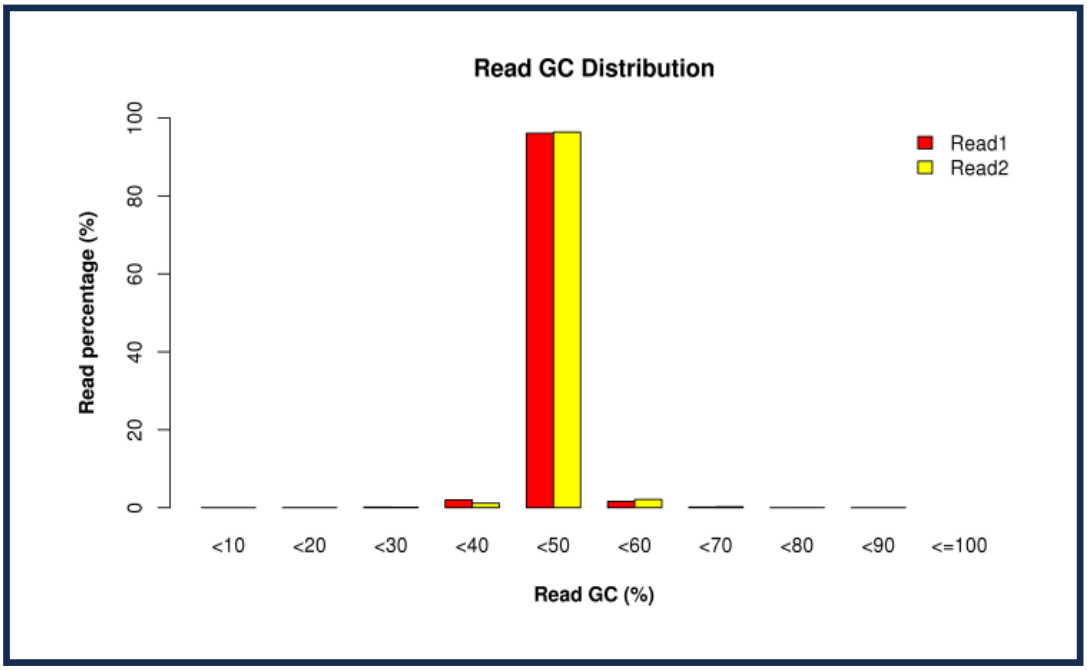

Figure 4.5.3. GC distribution plot of gut bacterial sequence reads from Sample P

V. Trimming of adapter and primer sequences:

Adapter and primer trimming of the raw read generated 54,569 reads from 64,500 reads in sample-C, 368,824 reads from 427,103 in sample-P and 69,928 reads from 79,716 in sample-T from total pair-end reads. A summary of trimmed consensus reads is shown in Table 4.7.

Table 4.7. Trimmed and consensus read summary

Sl. No.	Sample Name	Total Paired-end reads	Passed reads with primers	Total Consensus sequences
1	Sample C	64500	64500	54569
2	Sample T	79716	79716	69928
3	Sample P	427103	427103	368824

VI. Pre-processing of reads: chimera filter

A detailed result of the data after chimera filter carried out on individual sample is given in the Table 4.8.

Table 4.8. Pre-processing reads statistics

Sl. No.	Sample Name	Consensus sequences	Chimeric sequences	Pre-processed Consensus sequences
1	Sample C	54569	6983	47586
2	Sample T	69928	13174	56754
3	Sample P	368824	38494	330330

VII. Picking Operational taxonomic unit (OTUs), Classification and diversity analysis

A total of 15,926 OTUs were identified from 434,670 reads. From 15,926 total OTUs, 13,395 OTUs with less than 2 reads were removed and 2,531 OTUs were selected for further analysis (Table 4.9).

Table 4.9. Summary of OTUs

Total Pre-processed Consensus	434670
Total OTUs Picked	15926
Total Filtered OTUs (< 2reads)	13395
Total Filtered OTUs (after filtering <2 reads)	2531

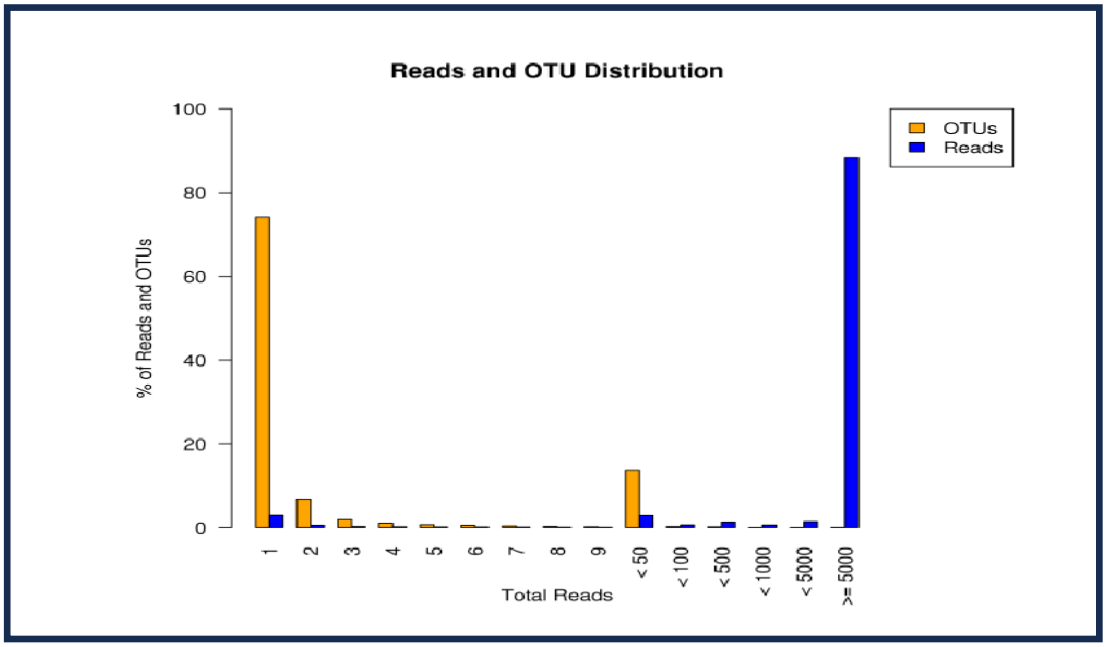

Figure 4.6. Bar plot representing the relative reads and OTUs proportion

The bar plots (Figure 4.6) shows a graphical representation of reads and OTU proportion. The blue bar represents percentage of total OTUs in the read-count groups. The orange bar represents percentage of total read contributed by the OTUs in the read-count group. The relative abundance plot at phylum, class, order, family, genus, and species level were analyszed based on the final filtered OTUs.

4.4.4. Gut bacterial community abundant study at different taxa level

A total of 2,531 Operational Taxonomic Units (OTUs) were processed and recorded five bacterial phyla *viz. Actinobacteria*, *Bacteroidetes*, *Proteobacteria*, *Verrucomicrobia* and *Firmicutes* in all the three sampled groups respectively (Figure 4.7.1). The phylum *Proteobacteria* represented the most dominant phyla in all the samples: Sample C (69.84%), Sample P (65.12%) and Sample T (69.15%), followed by the phylum *Firmicutes* (25.65%, 21.49% and 28.37% respectively) and phylum *Actinobacteria* (1.04%, 1.75% and 1.77% respectively). All other phyla including *Bacteroidetes*, *Verrucomicrobia*, had an average abundance of less than 1% and 3.12% (Sample C), 8.75% (Sample P) and 0.17% (Sample T) of OTUs were unassigned/unknown.

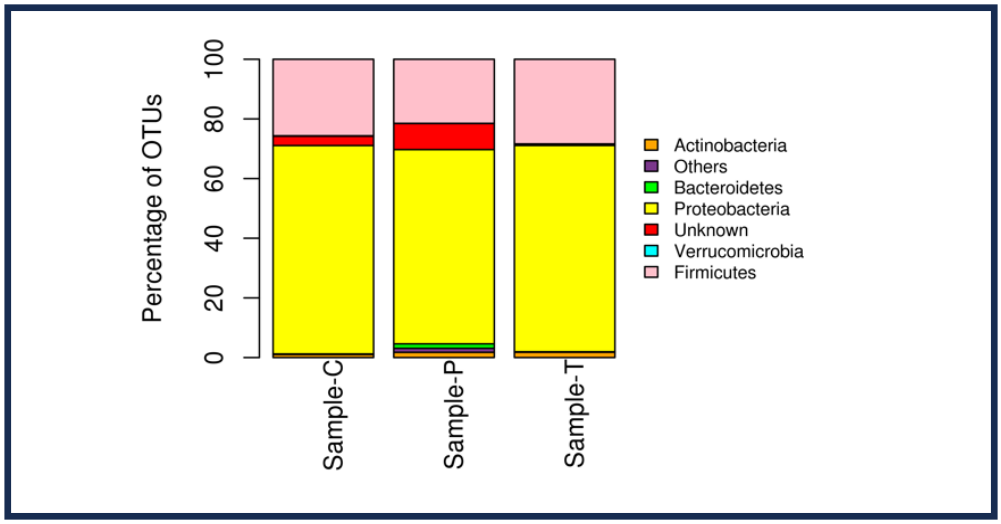

Figure 4.7.1. Relative abundance of bacterial OTUs at Phylum level

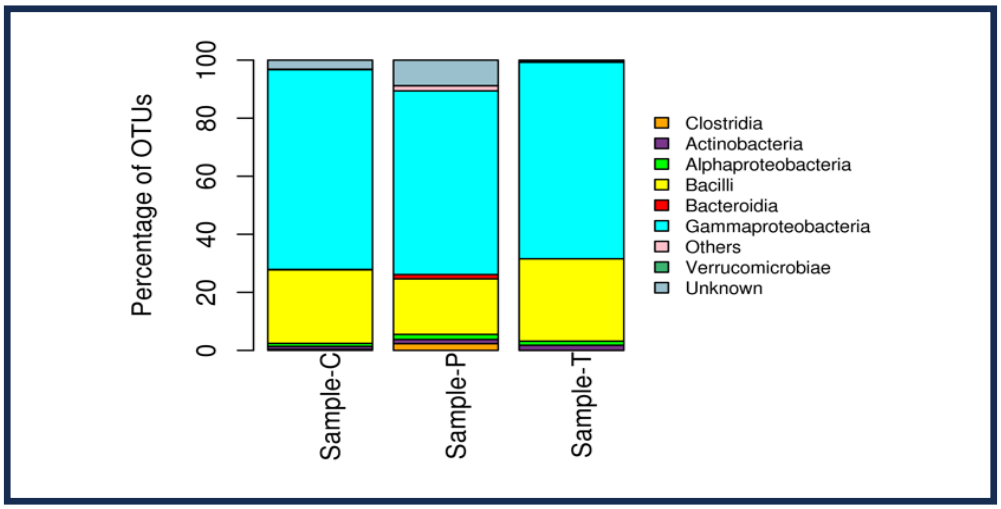

Figure 4.7.2. Relative abundance of bacterial OTUs at Class level

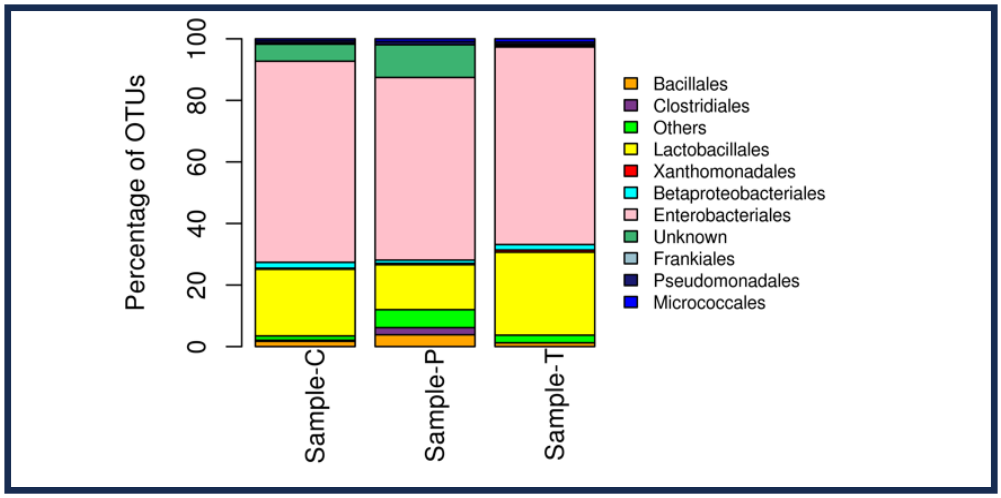

Figure 4.7.3. Relative abundance of bacterial OTUs at Order level

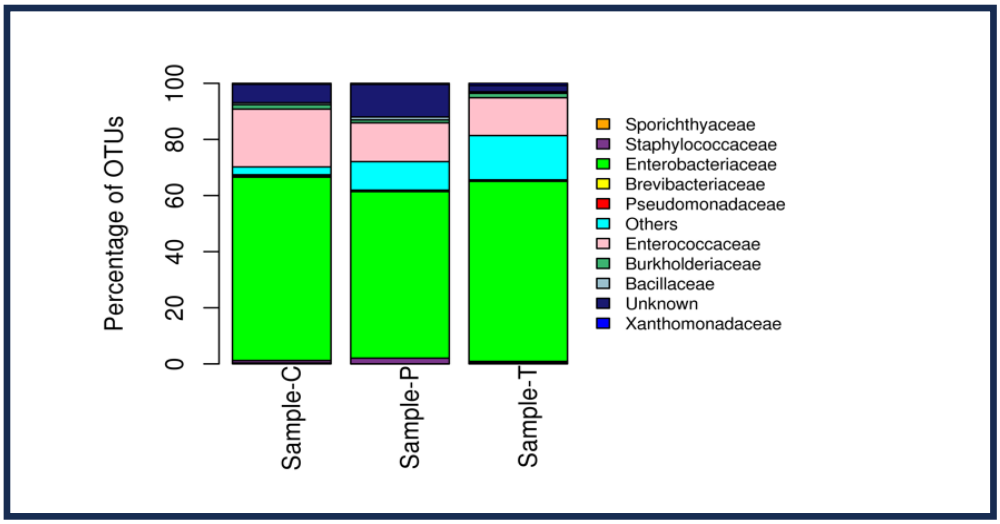

Figure 4.7.4.Relative abundance of bacterial OTUs at Family level

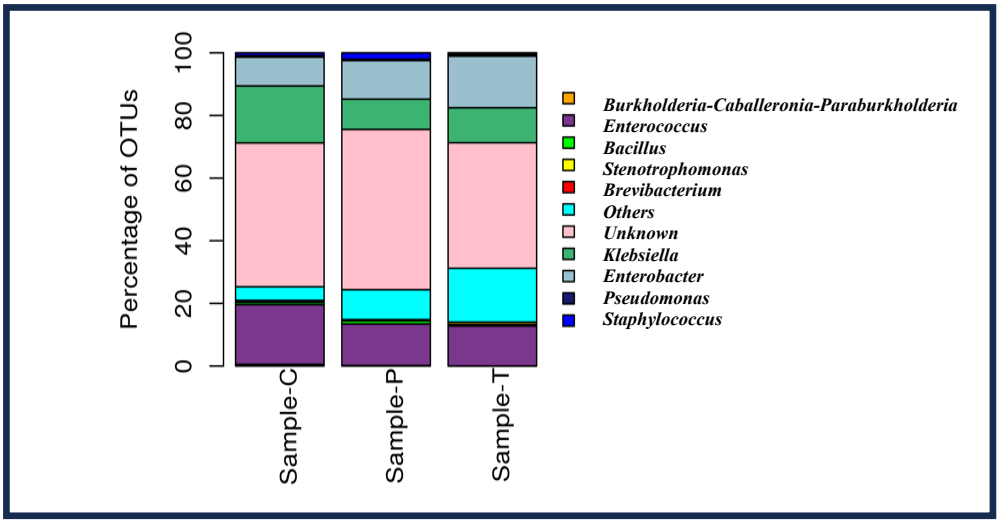

Figure 4.7.5. Relative abundance of bacterial OTUs at Genus level

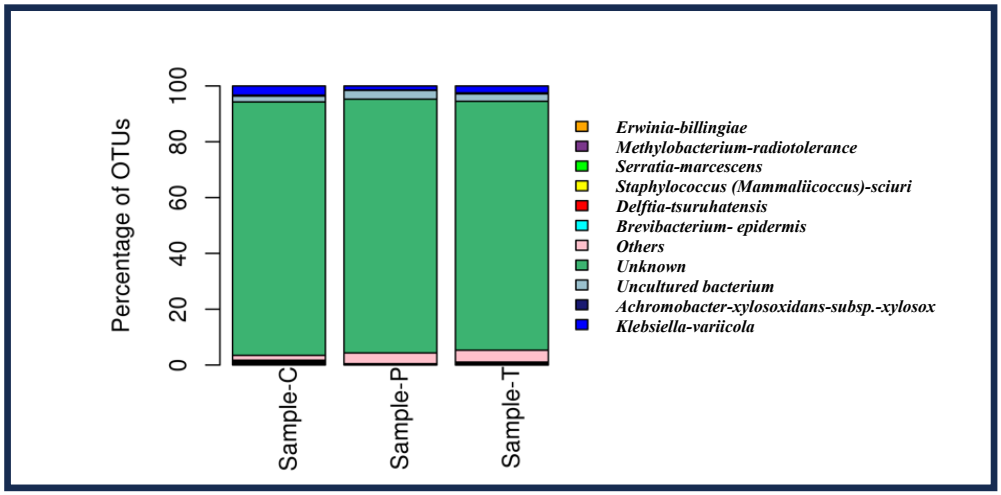

Figure 4.7.6. Relative abundance of bacterial OTUs at Species level.

Class level comparison recorded seven common bacterial orders with varying relative abundance in all the sampled groups (Figure 4.7.2). The most abundant class were Gammaproteobacteria (68.80% in Sample C, 63.28% in Sample P and 67.73%in Sample T) followed by Bacilli (25.30% in Sample C, 19.12% Sample P and 28.37% in Sample T). In Sample P, 8.79%, in Sample C 3.11% and in Sample, T 0.35% of unknown OTUs were recorded at class level.

At order level, nine known bacterial orders were recorded *viz.* Bacillales, Clostridiales, Lactobacillales, Xanthomonadales, Betaproteobacterials, Enterobacterials, Frankiales, Pseudomonas, Micrococcales (Figure 4.7.3). Enterobacteriales constitutes the most dominant order in all the samples 65.34% in Sample C, 59.34% in Sample P and 64.18% in Sample T. Lactobacillales was also found to be dominant next to Enterobacteriales being highest in Sample T (26.95%) followed by Sample C (21.66%) and Sample P (14.62%). In addition, Bacillales, Clostridiales, Xanthomonadales, Betaproteobacteriales, Frankiales and Pseudomonadales were the less dominant orders that were observed in all samples. The percentage of Unknown and Others OTUs were recorded highest in Sample P (10.69% and 5.8%) followed by 5.5% and 1.39% in Sample C and 0.53% and 2.48% in Sample T.

In all the three samples, *Enterobacteriaceae* (65.34% in Sample C, 64.18% in Sample T and 59.34% in Sample P), and *Enterococcaceae* (20.62% in Sample C, 13.83% in Sample P and 13.47% in Sample T) were found to be the most dominant families (Figure 4.7.4). Families including *Sporichthyaceae*, *Brevibacteriaceae*, *Pseudomonadaceae*, *Xanthomonadaceae* were represented by less 1% abundance in all the three groups. *Burkholderiaceae* showed an abundance of 1-2% in the three samples under study. This study also recorded nine known bacterial genus: *Burkholderia, Caballeronia-Paraburkholderia, Enterococcus, Bacillus, Stenotrophomonas, Brevibacterium,* and *Klebsiella*.

The most abundant genera were *Enterococcus* (19.06% in Sample C, 13.26% in Sample P, and 12.76% in Sample T), *Klebsiella* (18.19% in Sample C, 11.17% in Sample T and 9.67% in Sample P) and *Enterobacter* (9.18% in Sample C, 12.29% in

Sample P and 16.49% in Sample T) while 45.93% (Sample C), 51.16% (Sample P) and 40.07% (Sample T) of the OTUs were unassigned and recorded as unknown (Figure 4.7.5).

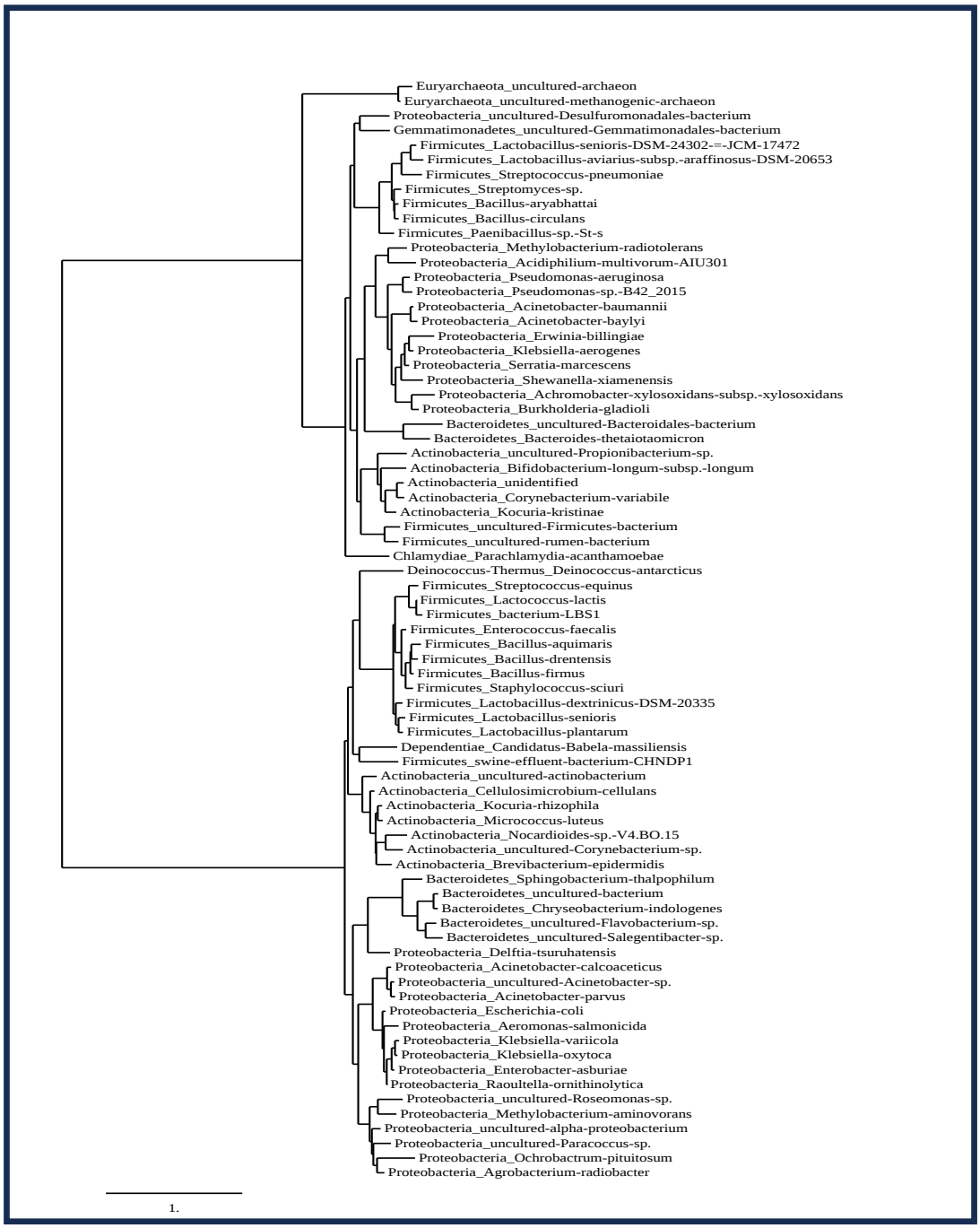

Figure 4.8. Combined phylogenetic tree of gut bacterial communities in all samples

At the species level, the analysis revealed a notable prevalence of unidentified bacterial taxa across all three samples - C (90.81%), P (90.94%), and T (89.18%). Furthermore, a distinct proportion of bacterial species, specifically 3.15% in Sample P, 2.07% in Sample C, and 2.65% in Sample T, comprised uncultured bacterial species. Conversely, a limited percentage of identified bacterial species were documented in all three samples, including *Erwinia-billingiae, Methylobacterium-radiotolerance, Serratia-marcescens, Staphylococcus (Mammaliicoccus) sciuri, Delftia-tsuruhatensis, Brevibacterium-epidermis, Achromobacter-xylosoxidans-subsp.-xylosox,* and *Klebsiella-variicola.* Remarkably, *Klebsiella variicola* exhibited the highest occurrence among all bacterial species, constituting 3.29% in Sample C, 2.48% in Sample T, and 1.48% in Sample P, respectively (Figure 4.7.6). The phylogenetic tree generated showed diverse gut bacterial population and evolutionary relationship among different bacterial taxa (Figure 4.8).

4.4.5. Visualization of Krona image

The Krona plot provided a comprehensive overview of the distribution of bacterial communities at various taxonomic levels within two dominant Phylum *i.e* Proteobacteria and Firmicutes. In Sample C, under the phylum Proteobacteria, the dominant genus was identified as *Enterobacter* (46%) and within the phylum Firmicutes, genus *Enterococcus* constituted 51% of the dominant taxa. This indicates a notable abundance of genus *Enterobacter* and *Enterococcus* within the sample, highlighting the diversity of bacterial populations. Sample T exhibited a distinct profile with Proteobacteria phylum populated by *Enterobacter* (41%), emphasizing a pronounced dominance of this genus in this sample. Furthermore, 41% of *Lactococcus-lactis* was observed under the phylum Firmicutes, suggesting presence of different genus across different phylum. In contrast, Sample P displayed a more diverse distribution of bacterial populations. Under the phylum Proteobacteria, *Enterobacter* accounted for 77%, and *Enterococcus* represented 17%. Additionally, the result revealed the presence of *Enterococcus* within the Firmicutes phylum, constituting 14% of the dominant taxa also recorded genus *Staphylooccus* with 2% (Figure 4.9).

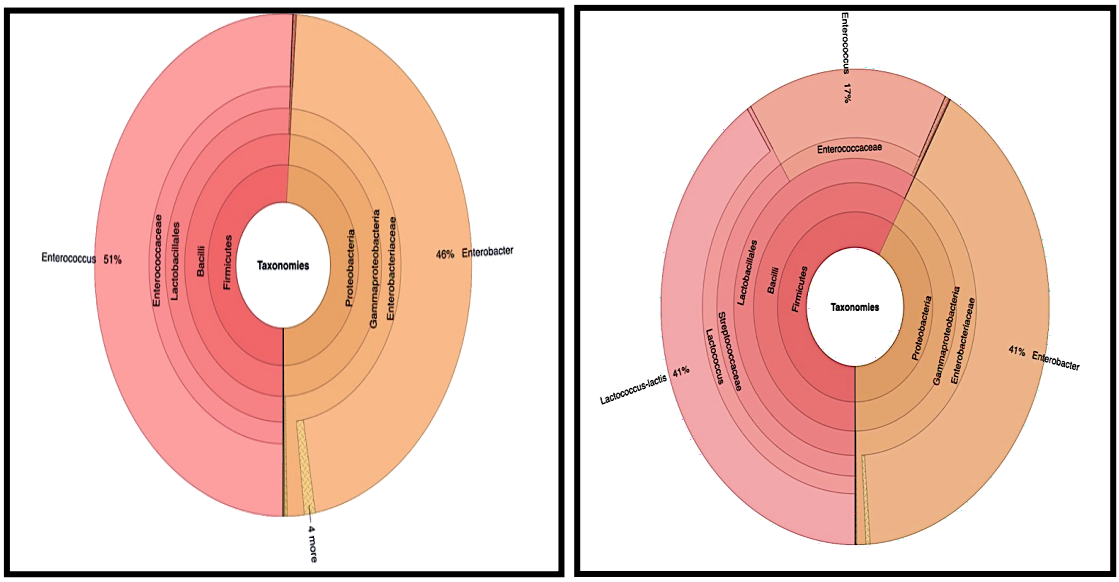

A. B.

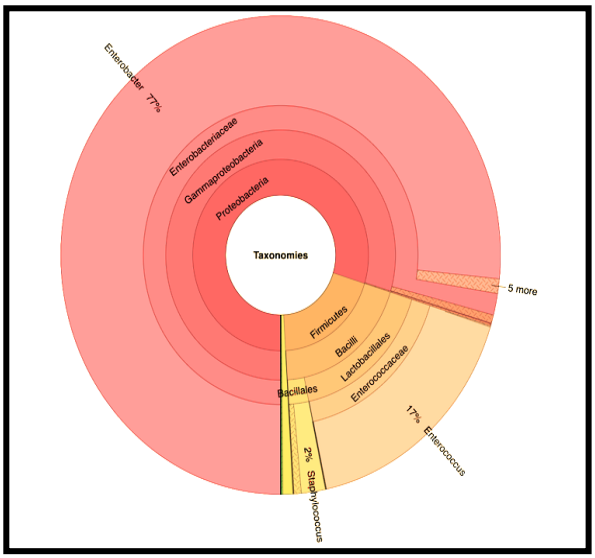

C.

Figure 4.9. Krona Plot of bacterial population of two dominant Phylum: A. Sample C; B. Sample T; C. Sample P

4.4.6. Alpha diversity analysis and rarefaction curves

The microbial diversity analysis within the samples was analysed by calculating Shannon, Chao1 and observed species metrics. The Shannon metrics indicated that Sample T showed more species richness and evenness than Sample P and Sample C. However, Chao1 metric results showed that in terms of unique OTUs, Sample P, have a

significant number of more unique OTUs than Sample C and Sample T. Similarly, the rarefaction curve of the observed species showed that the highest numbers of species were observed in Sample P with increasing number of observed species with each increasing x value, followed by Sample T and Sample C (Figure 4.10).

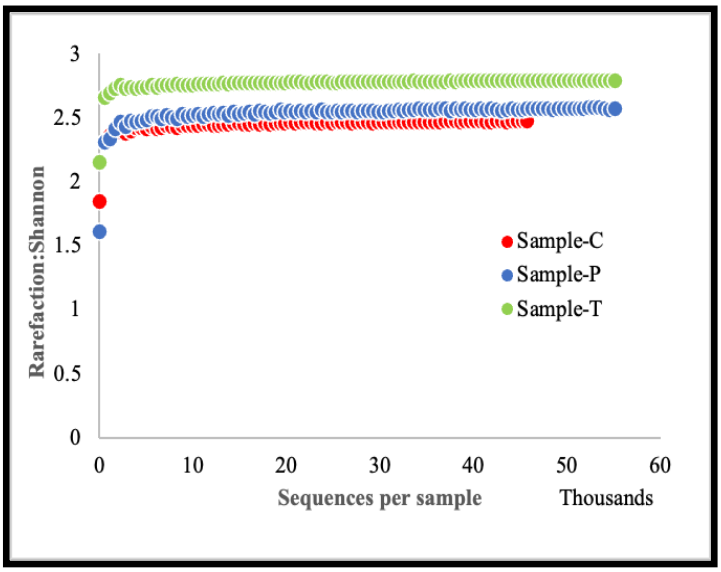

A.

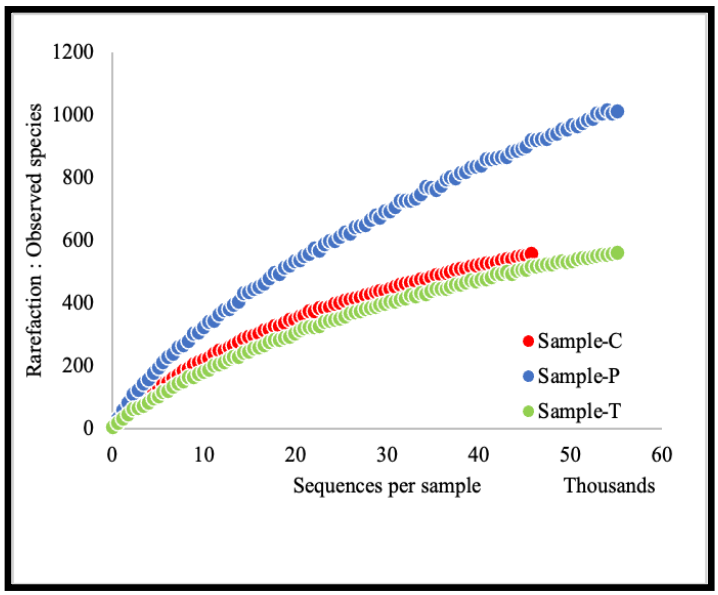

B.

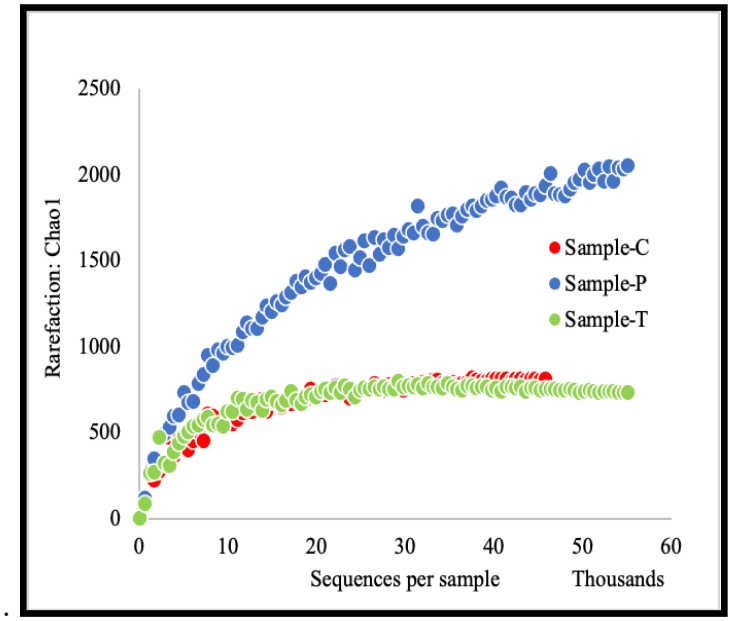

C.

Figure 4.10. Alpha diversity index curves for all three samples: A. Shannon rarefaction curve; B. Observed species rarefaction curve; C. Chao1 rarefaction curve

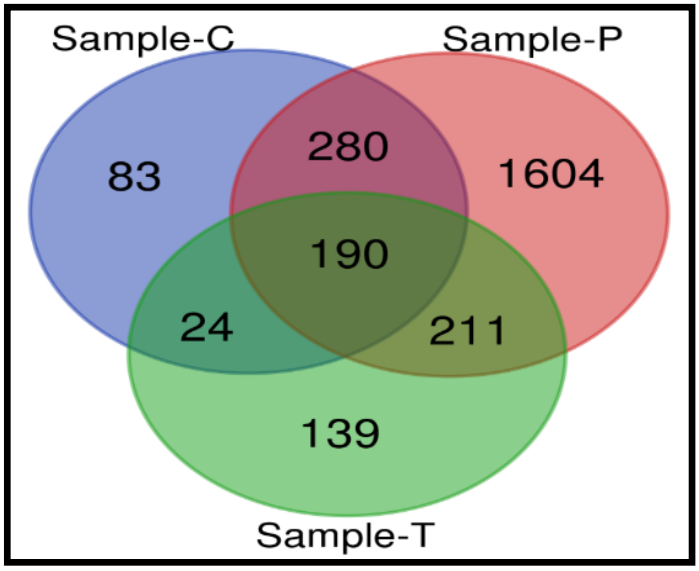

Figure 4.11. Comparative analysis of gut bacterial Operational Taxonomic Units (OTUs) in Venn diagram: showing shared and unique OTUs across samples C, T, and P.

4.4.7. Study of shared and unshared OTUs between groups using Venn diagram

Venn diagram the relationship between bacterial composition present in the three gut samples. In the similarity analysis out of total 2531 OTUs selected from all the sample group only 190 OTUs were showing common or similarities between all the

three samples whereas the number of unique genera recorded in Sample C, P and T were 83, 1604 and 139 respectively (Figure 4.11). The calculated similarity index based on shared OTU data of all three samples, recorded Sample C and T with highest similarity index (0.37) than Sample C and P (0.33) and Sample P and T (0.28). The similarity index report indicated that Sample C and T are more similar to each other than Sample P.

4.4.8. Co- Occurrence analysis of gut bacterial genera

Co-occurrence measurement in Sample C most connected bacterial genus recorded were *Klebsiella, Enterococcus, Enterobacter, Delftia, Serratia, Burkholderia-Caballeronia-Paraburkholderia, Pseudomonas, Bacillus and Staphylococcus.* In Sample T mostly connected genus were *Lactobacillus, Enterococcus, Lactococcus, Enterobacter, Bacillus, Stenotrophomonas, Staphylococcus, Serratia* and *Klebsiella,* whereas in Sample P the core bacterial genus recorded were *Staphylococcus, Enterococcus, Enterobacter, Brevundimonas, Stenotrophomonas, Serratia, Acinetobacter, Bacillus* and *Klebsiella*. In all the three samples the genus *Klebsiella, Enterococcus, Serratia, Bacillus* and *Staphylococcus* were present as core bacterial genus in the gut of *S. ricini* larvae (Figure 4.12).

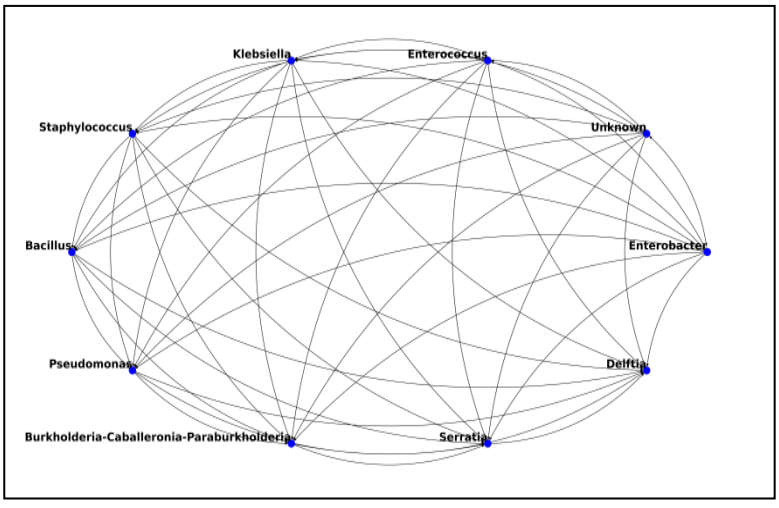

A.

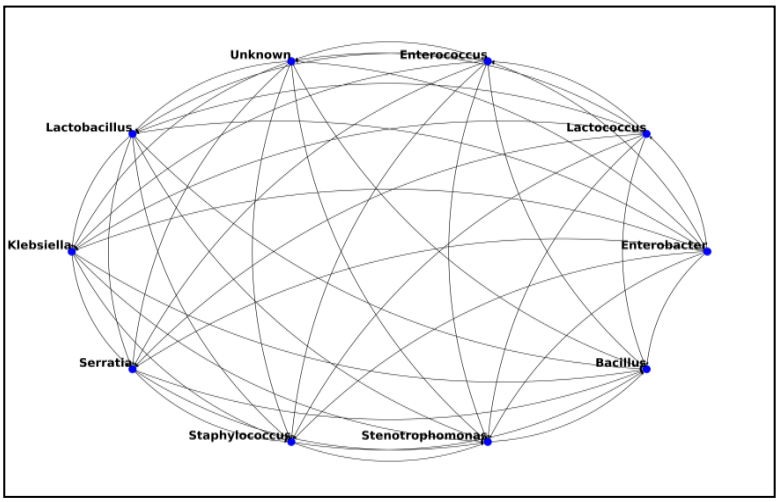

B.

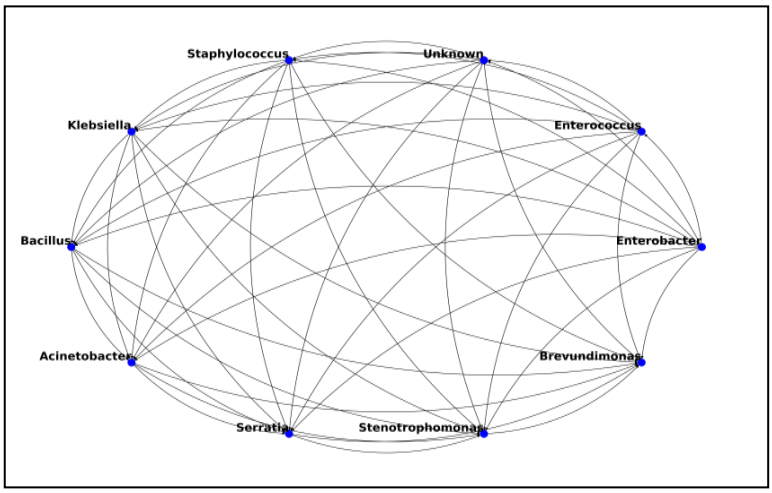

C.

Figure 4.12. Co-occurrence analysis of gut bacterial genera in gut samples: A. Sample C; B. Sample T; C. Sample P

4.4.9. Principal co-ordinate analysis (PCoA)

The result of principal coordinate analysis (PCoA) of all the three sample i.e C, T and P recorded that PC1 explained 92.1% variation in the data, while PC2 explained 7.9%. The PCoA plot revealed differences in the characteristics of the samples along the PC1 axis, suggesting that this axis is important in distinguishing between the samples. Each data point in the diagram signifies a sample, and the distance between these points illustrates the extent of variation among the samples (Figure 4.13).

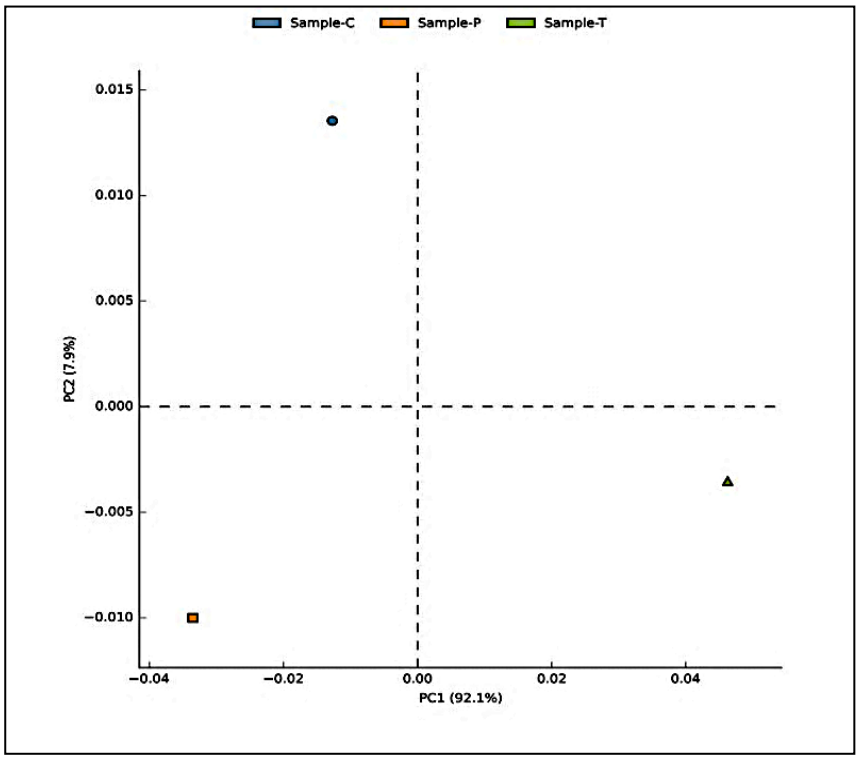

Figure 4.13. Principal Coordinate Analysis (PCoA) between Samples: C, T and P,

4.4.10. Functional annotation of gut bacterial genome

Functional annotation of *S. ricini* gut bacteria using KEGG pathway analysis recorded six types of functinal pathways in Level 1 metabolism, environmental information processing, genetic information processing, cellular processes, organismal systems, and human diseases (Figure 4.14.1). Role in metabolism recorded highest in all samples of *S. ricini* fed on three different sampled food plants. In the metabolism pathway, Sample T exhibits the highest percentage at 44.67%, closely followed by Sample C at 44.31%, while Sample P shows a slightly lower percentage at 43.70%. Moving to Environmental Information Processing, Sample C leads with the highest percentage at 21.21%, followed by Sample P at 21.20%, and Sample T at 18.73%.

Within the Unclassified category, Sample T has the highest percentage at 16.84%, followed by Sample P at 16.21%, and Sample C at 15.75%. In genetic information processing pathways, Sample T takes the lead with 16.07%, followed by Sample C at 15.43%, and Sample P at 14.97%. For cellular processes, Sample C records the lowest percentage at 1.88%, followed by Sample T at 2.22%, and Sample P at

2.44%. The human diseases and, organismal systems pathways exhibit minimal variations, emphasizing a relatively consistent distribution across the three samples.

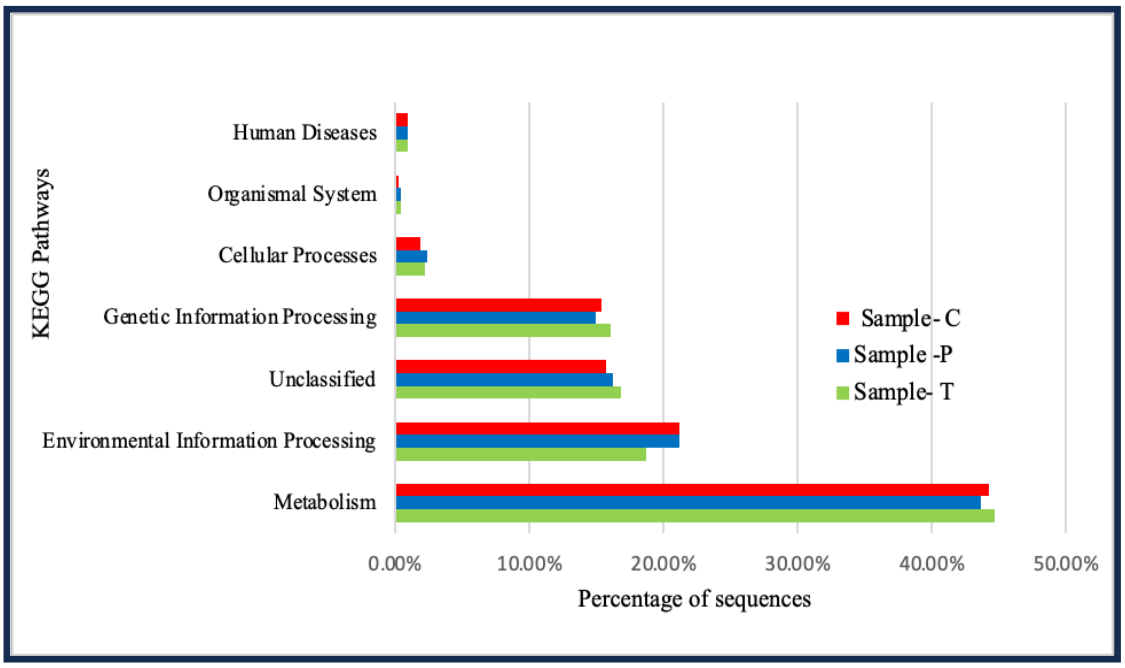

Figure 4.14. 1. Comparison of KEGG functional predictions in the gut bacterial communities of *S. ricini* fed on different host plants Level 1- Overall functional pathways

Furthermore the Level-2 Picrust analysis elucidates the distribution of functional gene categories within the gut bacteria of Samples T, P, and C across various KEGG pathways (Figure 4.12.2). Notably, in the membrane transport pathway, Sample C exhibits the highest percentage at 18.73%, followed by Sample P at 18.59%, and Sample T at 16.51%. Carbohydrate metabolism displays a gradual increase from Sample T (10.58%) to Sample C (11.51%), with Sample P at 10.64%. Amino acid metabolism follows a similar trend, with Sample T having the highest percentage at 8.54%, followed by Samples P (8.30%) and C (8.20%). In replication and repair, Sample T leads with 7.31%, followed by Sample C at 6.34%, and Sample P at 6.16%. The Poorly Characterized pathway shows marginal differences, with Sample P having the highest percentage at 5.53%, followed by Samples C (5.43%) and T (5.47%).

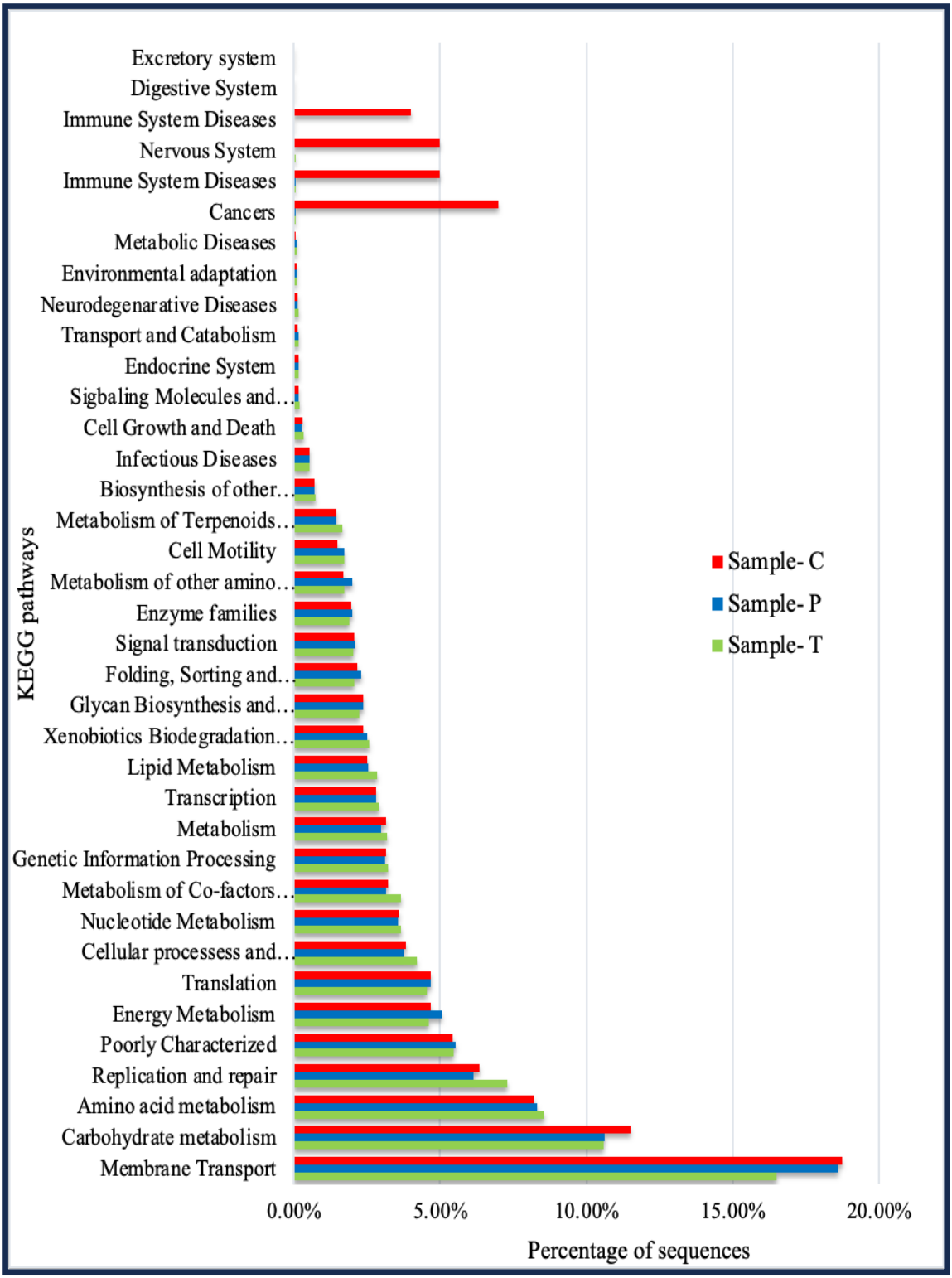

Figure 4.14. 2. Comparison of KEGG functional predictions in the gut bacterial communities of *S. ricini* fed on different host plants Level 2- analysis of metabolic pathways

Energy metabolism, translation, and cellular processes and signaling pathways exhibit variations across the three samples. Energy metabolism is slightly higher in Sample P (5.05%) compared to Sample T (4.61%) and Sample C (4.69%). Translation percentages are relatively consistent, with Sample T rcorded with 4.55%, and Samples P and C at 4.69%. Cellular processes and signaling show higher percentages in Sample T (4.21%) compared to Sample C (3.83%) T and Sample P (3.75%). Nucleotide metabolism and metabolism of co-factors and vitamins demonstrate subtle differences among the Samples, with Sample T leading in both pathways.

Genetic information processing pathways, encompassing transcription and metabolism, show comparable percentages across all samples. Lipid metabolism, xenobiotics biodegradation, glycan biosynthesis and metabolism display variations, emphasizing sample-specific functional characteristics. Furthermore the other metabolism pathway shows distinct percentages in each sample, with Sample T leading at 3.18%, followed by Sample C at 3.15%, and Sample P at 3.00%.

Based, on Level-3 KEGG pathway analysis, the guts of the Eri silkworm fifth instar larvae reared on different plants different hosts were recorded enriched with different functional proteins such as peptide/nickel transport system permease protein, ATP binding proteins, substrate binding protein, iron complex outer membrane receptor protein, also includes peptides, nickel, iron complex, sulfonate/nitrate/taurine, simple sugars, and polar amino acids transport system permease proteins.

Additionally, we identified the presence of enzymes such as F420H(2)-dependent quinone reductase and transketolase, glucose 6 phosphatase as well as regulatory proteins such as Lac I family transcription regulator and cold shock protein (beta-ribbon, CspA family) were identified in this study (Figure 4.14.3).

4.4.11. Statistical Analysis of Metagenomics Profile (STAMP)

Further statistical analysis recorded significance variation in proportion of functional proteins in groups. Result recorded the prevalence of the Peptide/Nickel Transport System Permease Protein in Sample P, with a significantly higher proportion

of sequences (12%) compared to Sample T(11.56%) and Sample C (10.50%), underscoring the distinctive protein expression profile in Samples (Figure 4.14.4). F420H(2)-Dependent Quinone Reductase and Sucrose 6 Phosphatase exhibited notable variation across samples, with Sample T demonstrating the highest expression levels, followed by Sample C, while Sample P exhibited the lowest proportions.

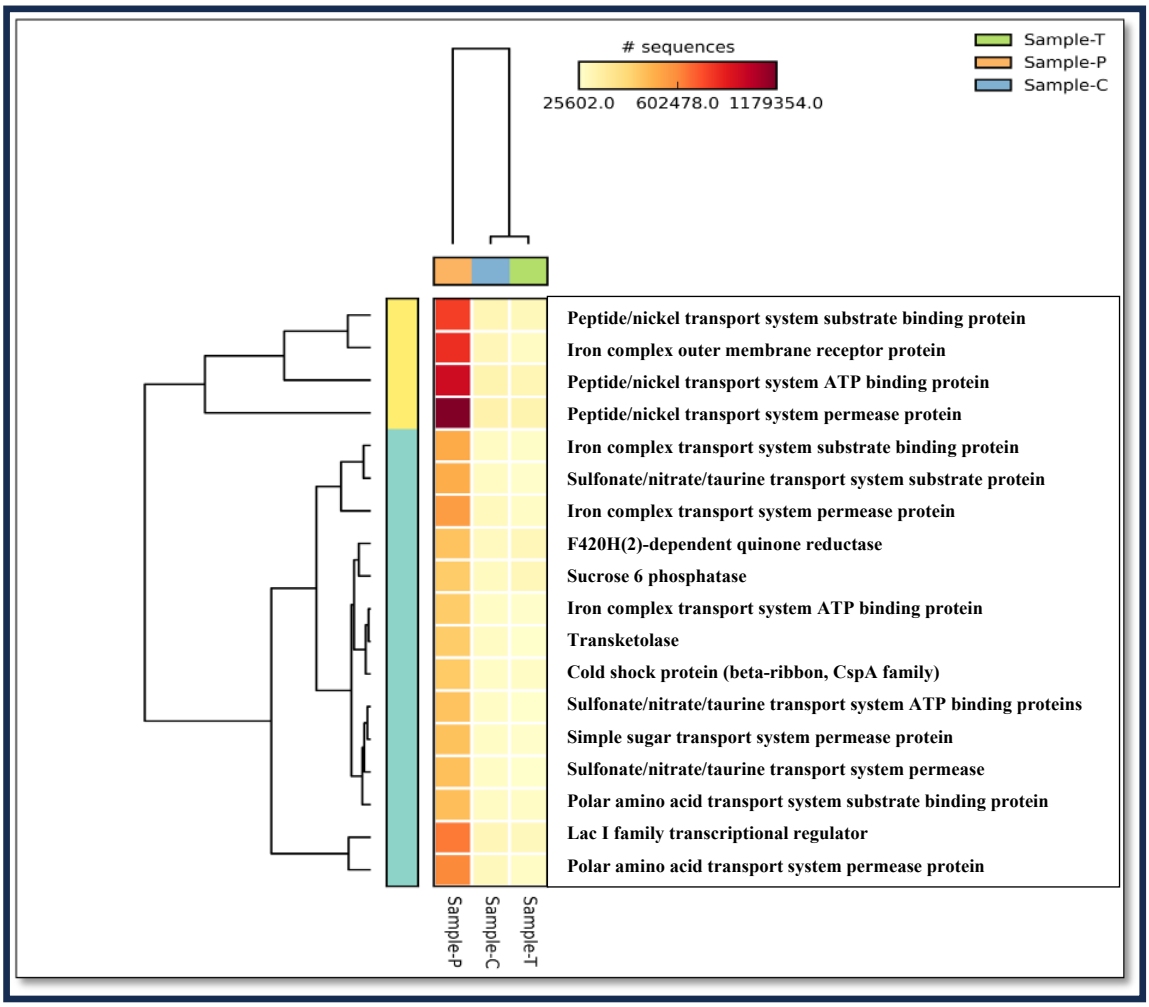

Figure 4.14.3. Heatmap showing comparison of KEGG functional predictions in the gut bacterial communities of *S. ricini* fed on different host plants Level 3- analysis of functional proteins

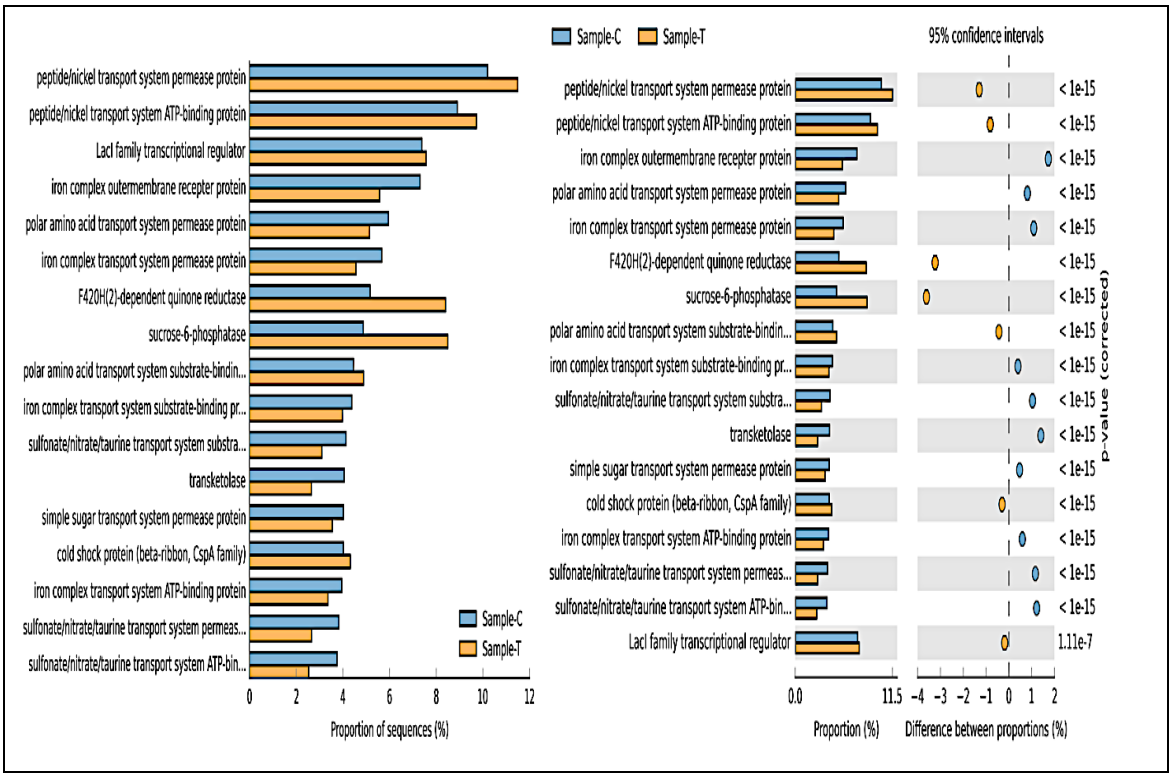
Sample-C
Sample-T
95% confidence intervals
peptide/nickel transport system permease protein
peptide/nickel transport system ATP-binding protein
LacI family transcriptional regulator
iron complex outermembrane recepter protein
polar amino acid transport system permease protein
iron complex transport system permease protein
F420H(2)-dependent quinone reductase
sucrose-6-phosphatase
polar amino acid transport system substrate-bindin...
iron complex transport system substrate-binding pr...
sulfonate/nitrate/taurine transport system substra...
transketolase
simple sugar transport system permease protein
cold shock protein (beta-ribbon, CspA family)
iron complex transport system ATP-binding protein
sulfonate/nitrate/taurine transport system permeas...
sulfonate/nitrate/taurine transport system ATP-bin...
< 1e-15
1.11e-7
p-value (corrected)
0 2 4 6 8 10 12
Proportion of sequences (%)
0.0 11.5
Proportion (%)
−4 −3 −2 −1 0 1 2
Difference between proportions (%)

A.

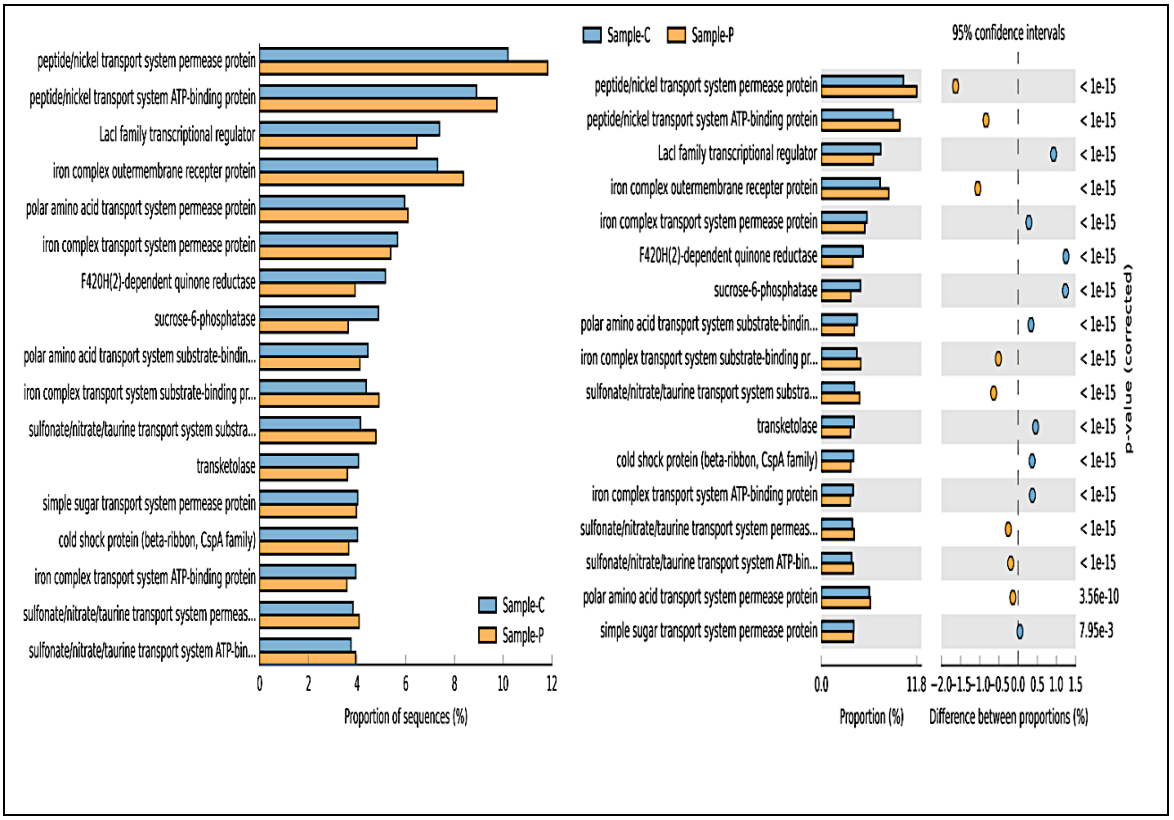
Sample-C
Sample-P
95% confidence intervals
peptide/nickel transport system permease protein
peptide/nickel transport system ATP-binding protein
LacI family transcriptional regulator
iron complex outermembrane recepter protein
polar amino acid transport system permease protein
iron complex transport system permease protein
F420H(2)-dependent quinone reductase
sucrose-6-phosphatase
polar amino acid transport system substrate-bindin...
iron complex transport system substrate-binding pr...
sulfonate/nitrate/taurine transport system substra...
transketolase
cold shock protein (beta-ribbon, CspA family)
iron complex transport system ATP-binding protein
sulfonate/nitrate/taurine transport system permeas...
sulfonate/nitrate/taurine transport system ATP-bin...
polar amino acid transport system permease protein
simple sugar transport system permease protein
< 1e-15
3.56e-10
7.95e-3
p-value (corrected)
0 2 4 6 8 10 12
Proportion of sequences (%)
0.0 11.8
Proportion (%)
−2.0 −1.5 −1.0 −0.5 0.0 0.5 1.0 1.5
Difference between proportions (%)

B.

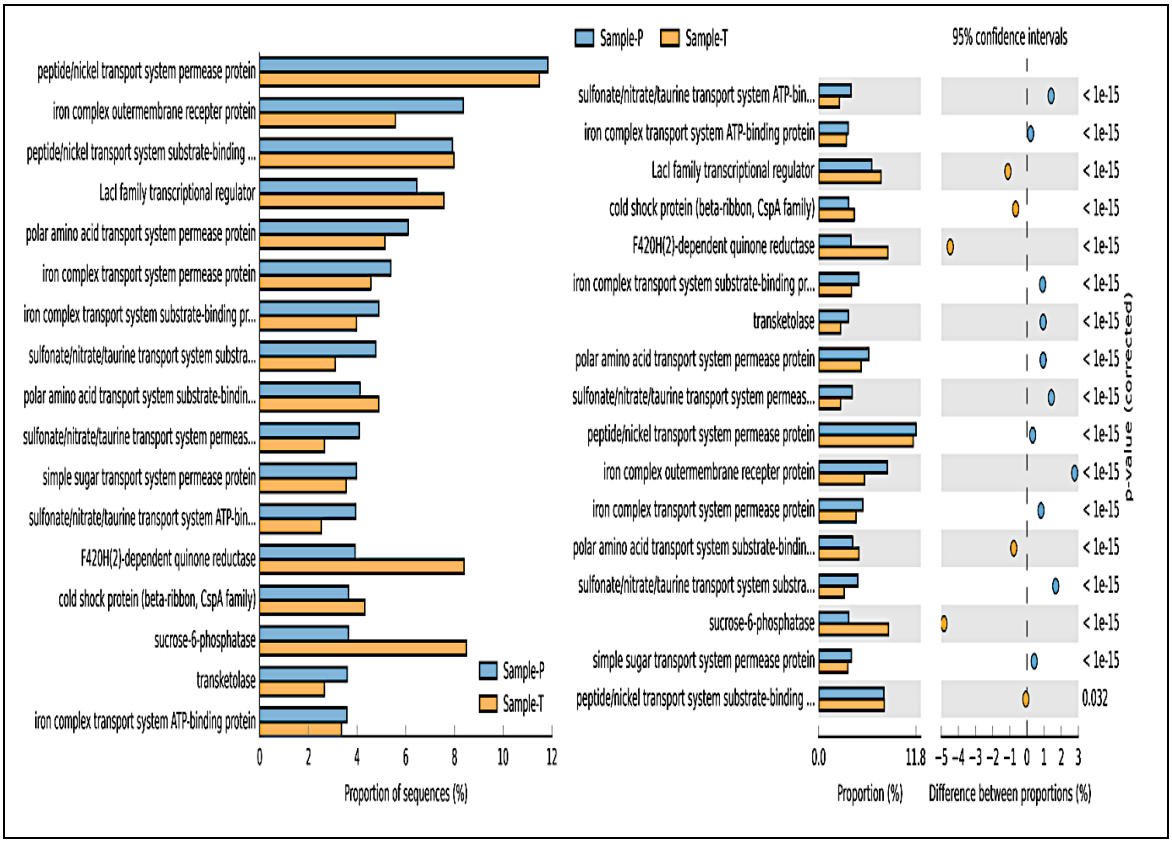

C.

Figure 4.14.4. Comparative analysis of KEGG pathway predicted functional proteins using STAMP Bar Plots with Extended Error Bars Illustrating Level 3 comparisons between samples: A. Sample C and T; B. Sample C and P; C. Sample P and T. The differences in percentage proportions between Sample T and C exceeded 3%, while Samples T and P, as well as Samples C and P, showed variations exceeding 4% and 1.5%, respectively

Several functional proteins, including Peptide/Nickel Transport System ATP Binding Protein, Iron Complex Outer Membrane Receptor Protein, Peptide/Nickel Transport System Substrate Binding Protein, Lac I Family Transcriptional Regulator, Polar Amino Acid Transport System Permease Protein, displayed moderate proportions across all three samples, contributing to a stable and consistent expression pattern within the dataset.

4.5. Isolation and characterization of some beneficial gut bacteria using a culture dependent method

4.5.1. Isolation of gut bacteria

A standard plate with equal dilution factor culture plates were taken from all three groups**.** A total of twenty gut bacterial colonies *i.e.* seven colonies from the gut of *S. ricini* reared on castor food plants, seven colonies from the gut of tapioca fed larvae and a total of six colonies from the gut of *S. ricini* larvae on papaya food plants (PLATE 5, 8), were taken for further screening test of colonies for digestive enzyme production.

4.5.2. Qualitative screening of digestive enzyme producing gut bacterial isolates

Out of twenty gut bacterial isolates screened for different digestive enzymes *viz.* α-amylase, cellulose, protease and lipase a total of fourteen isolates showed positive for digestive enzyme activity (Table. 4.10). All isolates screened positive for α-amylase activity (PLATE 6 A to I), ten isolates recorded positive for cellulase activities (PLATE 6 J to N), while positive proteinase activity is noted in seven isolates (PLATE 7 A to D).

Table 4.10. Qualitative screening of digestive enzyme activities of bacterial isolates

Name of Isolates	α - amylase	Cellulase	Proteinase	Lipase
C1	+	+	+	+
C2	+	+	+	+
C3	+	+	-	-
C4	+	-	-	+
C5	+	+	+	-
C6	+	-	-	+
T1	+	-	-	+
T2	+	+	+	-
T3	+	-	+	+
T4	w+	+	-	+
P1	+	+	-	-
P2	+	+	-	+
P3	w+	+	+	+
P4	w+	+	+	+

Where, (+) = Positive for enzyme activity, (-) = Negative for enzyme activity, (**w+**) = weak positive.

Positive lipase activity was observed in total ten isolates (PLATE 7 E to I). Notably, weak positive (W+) activity is seen in α-amylase for isolates T4, P3, and P4. The enzymatic profiles recorded the diverse functional attributes within the bacterial isolates from samples C, T, and P.

4.6. Phenotypic characterization of Enzyme producing isolates

4.6.1. Morphological characterization

The morphological traits of the bacterial isolates exhibited a wide range of characteristics (Table 4.11). Notably, isolate C3 displayed a rounded shape with a raised elevation, while T3 exhibited a yellow coloration and slightly convex elevation. The majority of isolates, such as C2, C4, C5, and C6, exhibited round shapes with varying sizes, elevations, and creamish colouring. Transparent opacity was observed in T2 and P1 isolates, with flat elevation. These isolates exhibit differences in opacity, ranging from opaque to translucent.

4.6.2. Physiological characteristics of isolates

The physiological characterization of bacterial isolates from samples C, T, and P revealed differences in various physical and biochemical traits (Table 4.12). In terms of Gram nature, Sample C contains Gram-positive cocci in bunches (C1 and C2), Gram-positive rods (C3), Gram positive cocci (C6), and Gram-negative rods (C4 and C5). Sample T exhibits Gram-positive cocci (T1 and T4) and Gram-positive rods (T2 and T3), while Sample P is characterized by Gram-negative rods (P1, P2, P3) and Gram positive cocci (P4) (PLATE 9). Catalase activity is uniformly present across all isolates from Samples C, T, and P.

Oxidase activity was present in most isolates except for C3 and C4 in Sample C. In Sample T isolates T1 and T4 showed positive oxidase activity while in sample P only isolate P4 showed positive for activity. The ability to produce KOH varies, with isolates in Samples C and T showing positive reactions, whereas Sample P exhibits mixed results. Tolerance to different pH levels (7, 6, 9, 10, and 11) is observed across all isolates, indicating a versatile pH tolerance. Similarly, the isolates demonstrate varying degrees of tolerance to different NaCl concentrations (0%, 2%, 4%, 6%, 8%, and 10%).

Table 4.11. Table showing morphological characteristics of isolates

Name of Isolates	Colony Morphological Characteristics of Isolates						
	Size	Shape	Colour	Margin	Elevation	Opacity	Consistency
C1	Pinpoint	Round	Creamish white	Entire	convex	Opaque	Smooth
C2	2-5 mm	Round	Cream	Entire	Convex	Opaque	Smooth
C3	2.8mm	Round	Cream	Entire	Raised	Opaque	Smooth
C4	2-5 mm	Round	Cream	Entire	Flat	opaque	smooth
C5	2-5 mm	Round	Cream	Entire	Convex	Opaque	Smooth
C6	2-5 mm	Round	Cream	Entire	Convex	Opaque	Smooth
T1	2-5 mm	Round	Cream	Entire	Convex	Opaque	Smooth
T2	pinpoint	Round	Cream	Entire	Flat	Transparent	Smooth
T3	pinpoint	Round	Yellow	Entire	Slightly Convex	Translucent	Smooth
T4	2.5mm	Round	Cream	Entire	Convex	Opaque	Smooth
P1	Pinpoint	Round	Cream	Entire	Flat	Transparent	Smooth
P2	2-5mm	Round	White	Entire	Flat	Opaque	Smooth
P3	2-3mm	Round	Cream	Entire	Convex	Opaque	Smooth
P4	1-2mm	Round	White	Entire	Convex	Opaque	Smooth

Table 4.12. Table showing Physiological characteristics of gut bacterial isolates

Physiological Characters	Bacterial Isolates													
	C1	C2	C3	C4	C5	C6	T1	T2	T3	T4	P1	P2	P3	P4
Gram nature	Gram + cocci in bunch	Gram + cocci in bunch	Gram + rods	Gram – rods	Gram – short rods	Gram + cocci	Gram + cocci	Gram + rods	Gram + rods	Gram + cocci	Gram – rods	Gram – rods	Gram – rods	Gram + cocci
Catalase	+	+	+	+	+	+	+	+	+	+	+	+	+	+
Oxidase	+	+	-	-	+	+	+	-	-	+	-	-	-	+
KOH	-	-	-	+	+	-	-	+	-	-	+	+	-	-
Tolerance to different pH														
7	+	+	+	+	+	+	+	+	+	+	+	+	+	+
6	+	+	+	+	+	+	+	+	+	+	+	+	+	+
9	+	+	+	+	+	+	+	+	+	+	+	+	+	+
10	+	+	+	+	+	+	+	+	+	+	+	+	+	+
11	+	+	-	w+	w+	+	+	W+	W+	+	+	+	+	+
Tolerance to different Nacl Concentration														
0%	+	+	+	+	W+	W+	-	+	-	W+	+	+	W+	W+
2%	+	+	+	+	+	+	+	+	W+	+	+	+	+	+
4%	+	+	+	W+	-	+	+	+	W+	+	+	+	+	+
6%	+	+	W+	W+	-	+	+	-	W+	+	+	+	+	+
8%	+	+	W+	-	-	+	+	-	W+	+	+	-	+	+

10%	+	+	**W+**	-	-	+	+	-	**W+**	+	**w+**	-	+	+
Tolerance to different Temperature														
5ºC	-	-	-	-	-	-	-	-	-	-	-	-	-	-
10ºC	-	-	-	-	-	-	-	-	-	-	-	-	-	-
20ºC	+	+	+	+	+	+	+	+	-	+	+	+	+	+
25ºC	+	+	+	+	+	+	+	+	+	+	+	+	+	+
37ºC	+	+	+	+	+	+	+	+	+	+	+	+	+	+
45ºC	+	+	+	-	-	-	**W+**	-	-	**W+**	-	**W+**	-	-

Substrate utilization Test														
ß-galactosidase	-	-	+	+	-	-	-	**W+**	+	-	**W+**	-	-	-
Arginine Dihydrolase	-	-	-	-	-	-	-	-	-	-	-	-	-	-
Lysine Decarboxylase	-	-	-	-	-	-	-	-	-	-	-	**W+**	-	-
Ornithine Decarboxylase	-	-	-	-	-	-	-	-	-	-	-	-	-	-
Citrate utilization	-	-	-	-	-	-	-	-	-	-	-	+	-	-
H_2S production	-	-	-	-	-	-	-	-	-	-	-	-	-	-
Urease	-	-	-	+	-	-	-	+	-	-	+	+	-	-
Tryptophane Deaminase	-	-	-	-	+	-	-	-	-	-	-	-	-	-

Indole production	-	-	-	-	-	-	-	-	-	-	-	+	-	-
acetoin production(Voges Proskauer)	-	**W+**	-	+	-	-	-	+	**W+**	-	+	+	-	-
Gelatinase	+	+	-	-	+	+	+	-	+	+	-	-	+	+
Fermentation/ oxidation of														
Glucose	+	+	**W+**	+	-	-	-	+	-	-	+	+	-	-
Mannitol	-	-	-	+	-	-	-	+	-	-	+	+	-	-
Inositol	-	-	-	+	-	-	-	+	-	-	+	+	-	-
Sorbitol	-	-	+	-	-	-	-	-	-	-	-	+	-	-
Rhamnose	-	-	-	-	-	-	-	-	-	-	-	+	-	-
Saccharose	-	-	**W+**	+	-	-	-	+	-	-	+	+	-	-
Melibiose	-	-	-	+	-	-	-	+	-	-	+	+	-	-
Amygdalin	-	-	-	-	-	-	-	-	-	-	**W+**	+	-	-
Arabinose	-	-	-	+	-	-	-	+	-	-	+	+	-	-

*(+) = Positive indicates presence of activity, (-) = Absence of activity, (**W+**) = Weakly present

Temperature tolerance varies among isolates, with most thriving at 20ºC, 25ºC, and 37ºC. Substrate utilization tests reveal differences in enzymatic activities, such as ß-galactosidase, urease, Voges-Proskauer, gelatinase, and fermentation/oxidation of specific sugars.

4.7. Study of some nutritionally important cultivable gut bacteria through quantitative enzymatic assay

All the enzyme activity result was calculated from the standard curve used for each enzyme assay (Figure 4.15).

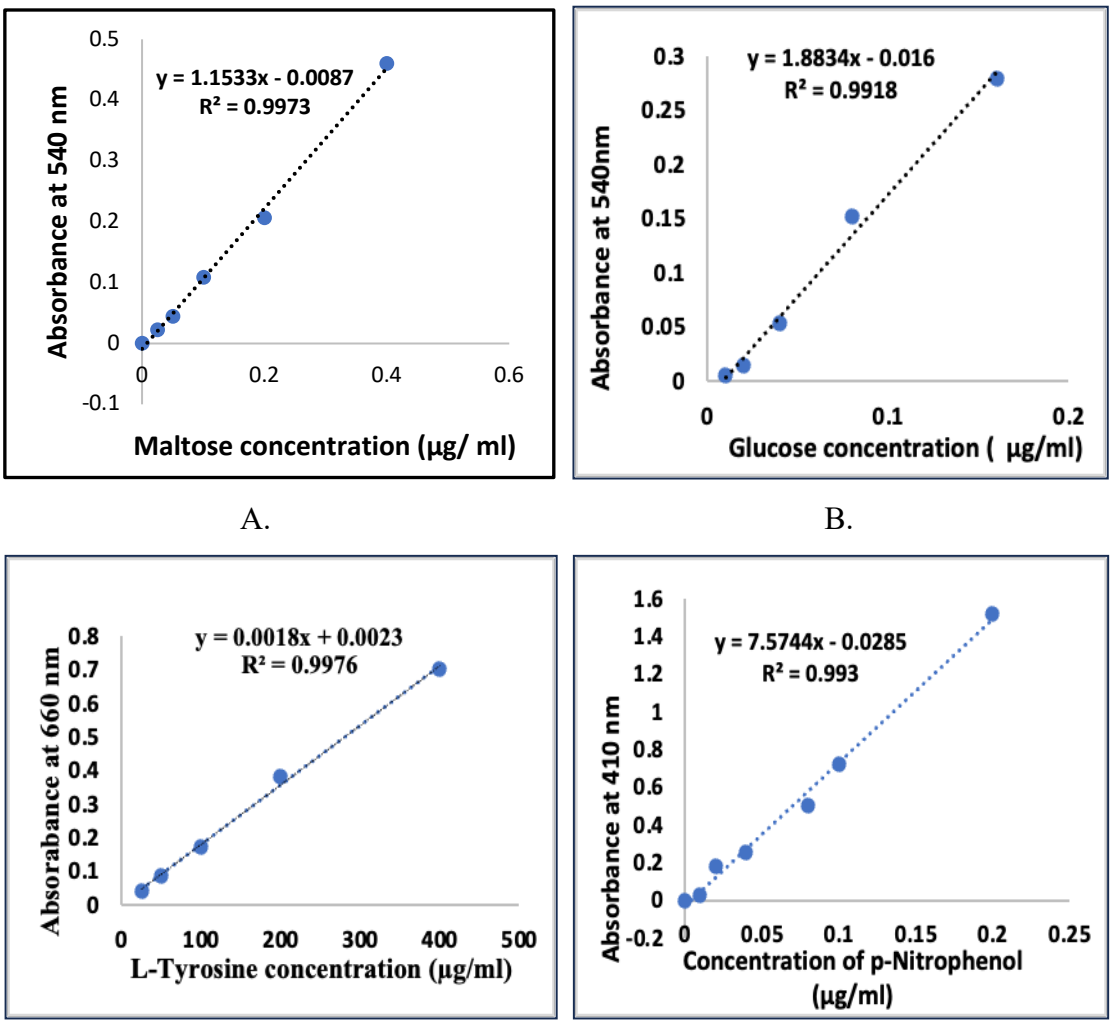

Figure. 4.15. Standard curves: A. Maltose standard curve for α-amylase; B. D-glucose standard curve for cellulose; C. L-Tyrosine standard curve for protease; D. p-Nitrophenol standard curve for lipase

I. α-amylase assay

The α-amylase activity of 14 positive isolates exhibited significant variation at the P<0.05 level. Among these isolates, C4 demonstrated the highest activity at 1.634±0.006 U/ml, closely followed by C5 (1.565±0.434 U/ml), C6 (1.138±0.169 U/ml), and T2 (1.152±0.157 U/ml). In contrast, T4 displayed the lowest α-amylase activity at 0.103±0.083 U/ml. These results highlight the variability in α-amylase production across the 14 isolates, indicating potential differences in their enzymatic capabilities (Table 4.13).

Table 4.13. Quantitative α- amylase enzyme activity of isolates

Sl. No.	Name of Isolates	α-amylase activity (U/ml)
1	C1	0.497±0.05
2	C2	0.463±0.05
3	C3	1.128±0.003
4	C4	1.634 ±0.006
5	C5	1.565±0.434
6	C6	1.138±0.169
7	T1	0.773±0.006
8	T2	1.152±0.157
9	T3	0.768±0.401
10	T4	0.103±0.083
11	P1	0.698±0.020
12	P2	0.366±0.068
13	P3	0.186±0.133
14	P4	0.276±0.060

Values are presented as Mean ± SE x t-score @ 95% CI, Means with significant differences at (P<0.05)

II. Cellulase enzyme assay

The cellulase activity of ten positive isolates was assessed, revealing significant variations (P≤0.05) in cellulase production among them (Table 4.14). Among the isolates, C5 exhibited the highest cellulase activity with a value of 0.104±0.038 U/ml, followed by T2 with 0.101±0.018 U/ml. C3 also demonstrated notable cellulase activity, recording 0.084±0.005 U/ml. On the other hand, P3 displayed the lowest cellulase

activity among the isolates, registering 0.025±0.003 U/ml. These suggested potential differences in their enzymatic capabilities

Table 4.14. Quantitative cellulase enzyme activity of isolates

Sl. No.	Name of isolates	Cellulase activity (U/ml)
1	C1	0.048±0.003
2	C2	0.049±0.025
3	C3	0.084±0.005
4	C5	0.104±0.038
5	T2	0.101±0.018
6	T4	0.045±0.011
7	P1	0.075±0.011
8	P2	0.034±0.020
9	P3	0.025±0.003
10	P4	0.059±0.036

Values are presented as Mean ± SE x t-score @ 95% CI, Means with significant differences at ($P<0.05$)

III. Proteinase enzyme assay

The results from the quantitative protease enzyme activity assay, recorded varying levels of enzyme activity among the isolates (Table 4.15). Notably, among all the proteinase-positive isolates, the highest proteinase enzyme activity was observed in the P3 isolate, with a recorded value of 0.619±0.350 U/ml followed by T2 with 0.569±0.011 U/ml, T3 with 0.555±0.159 U/ml and P4 with 0.532±0.050. Additionally, C5, C2, and C1 isolates displayed decreasing levels of enzyme activity, with C1 recording the least at 0.334±0.115 U/ml. These findings emphasize the distinct protease enzyme production profiles among the isolates, shedding light on the diversity in their enzymatic capabilities.

IV. Lipase assay

The results from the quantitative lipase enzyme activity assay, as presented in Table 4.16, showcase variations in lipase activity among the isolates. Notably, Isolate T1 isolated from the larval gut of Eri silkworm reared on tapioca food plant exhibited the highest lipase activity at 0.234±0.007 U/ml, followed by C4 with 0.202±0.018 U/ml and

P2 with 0.189±0.007 U/ml. Additionally, C1, C2, C6, T3, T4, and P3 isolates displayed lower lipase activities, with P4 isolate isolated from the castor fed larvae, recording the least at 0.103±0.007 U/ml. These findings highlight the diversity in lipase enzyme production across the isolates, underscoring potential differences in their enzymatic capabilities.

Table 4.15. Quantitative proteinase enzyme activity of isolates

Sl. No.	Name of isolates	Proteinase activity (U/ml)
1	C1	0.334±0.115
2	C2	0.355±0.081
3	C5	0.438±0.029
4	T2	0.569±0.011
5	T3	0.555±0.159
6	P3	0.619±0.350
7	P4	0.532±0.050

Values are presented as Mean ± SE x t-score @ 95% CI, Means with significant differences at ($P<0.05$)

Table 4.16. Quantitative lipase enzyme activity of isolates

Sl. No.	Name of Isolates	Lipase activity (U/ml)
1	C1	0.157±0.017
2	C2	0.151±0.026
3	C4	0.202±0.018
4	C6	0.131±0.021
5	T1	0.234±0.007
6	T3	0.144±0.013
7	T4	0.149±0.024
8	P2	0.189±0.007
9	P3	0.135±0.024
10	P4	0.103±0.007

Values are presented as Mean ± SE x t-score @ 95% CI, Means with significant differences at ($P<0.05$)

4.8. Molecular Identification of enzyme producing isolates

The molecular identification of gut bacterial isolates based on their gene sequencing data and NCBI Blast analysis result Isolate C1 was identified as *Mammaliicoccus sciuri*, with the GenBank accession ID OR016518. Isolate C2 belongs to the species *Mammaliicoccus sp.*, and its GenBank accession ID is OR828234. Isolate C3 was identified as *Bacillus licheniformis* (GenBank: OR739576), while Isolate C4 is classified as *Winslowiella sp*. with the GenBank accession OR963258. Isolate C5 is a *Brevundimonas diminuta* (GenBank: OR964999), and Isolate C6 is *Staphylococcus sp.* (GenBank: OR211560). From the Sample T- T1 corresponds to *Mammaliicoccus sp.* (GenBank: OR921980), T2 to *Bacillus sp.* (GenBank: OR976063), T3 to *Bacillus subtilis* (GenBank: OR923392), and T4 to another *Mammaliicoccus sciuri.* (GenBank: OR924301). Furthermore, P1 identified as *Winslowiella iniecta* (GenBank: OR945735), P2 as *Klebsiella oxytoca* (GenBank: OR958639), P3 as *Citrobacter sp.* (GenBank: OR976270), and P4 as *Mammaliicoccus sp.* (GenBank: OR958729) (Table 4.17).

Table 4.17.Molecular identification NCBI blast result of bacterial isolates

Sl. No.	Bacterial Isolates	Blast result.	GenBank accession ID
1.	ISOLATE-C1	*Mammaliicoccus sciuri*	GenBank OR016518
2.	ISOLATE-C2	*Mammaliicoccus sp.*	GenBank OR828234
3.	ISOLATE-C3	*Bacillus licheniformis*	GenBank OR739576
4.	ISOLATE-C4	*Winslowiella sp.*	GenBank OR963258
5	ISOLATE-C5	*Brevundimonas diminuta*	GenBank OR964999
6	ISOLATE-C6	*Staphylococcus sp.*	GenBank OR211560
7	ISOLATE-T1	*Mammaliicoccus sp.*	GenBank OR921980
8	ISOLATE-T2	*Bacillus sp.*	GenBank OR976063
9	ISOLATE-T3	*Bacillus subtilis*	GenBank OR923392
10	ISOLATE-T4	*Mammaliicoccus sciuri*	GenBank OR924301
11	ISOLATE-P1	*Winslowiella iniecta*	GenBank OR945735
12	ISOLATE-P2	*Klebsiella oxytoca*	GenBank OR958639
13	ISOLATE-P3	*Citrobacter sp.*	GenBank OR976270
14	ISOLATE-P4	*Mammaliicoccus sp.*	GenBank OR958729

4.9. Phylogenetic tree of Bcaterial Isolates

Phylogenetic analysis has elucidate the evolutionary relationships between the gut bacterial isolates isolated from the present study and their closest relatives forming different clades (Figure 4.16).

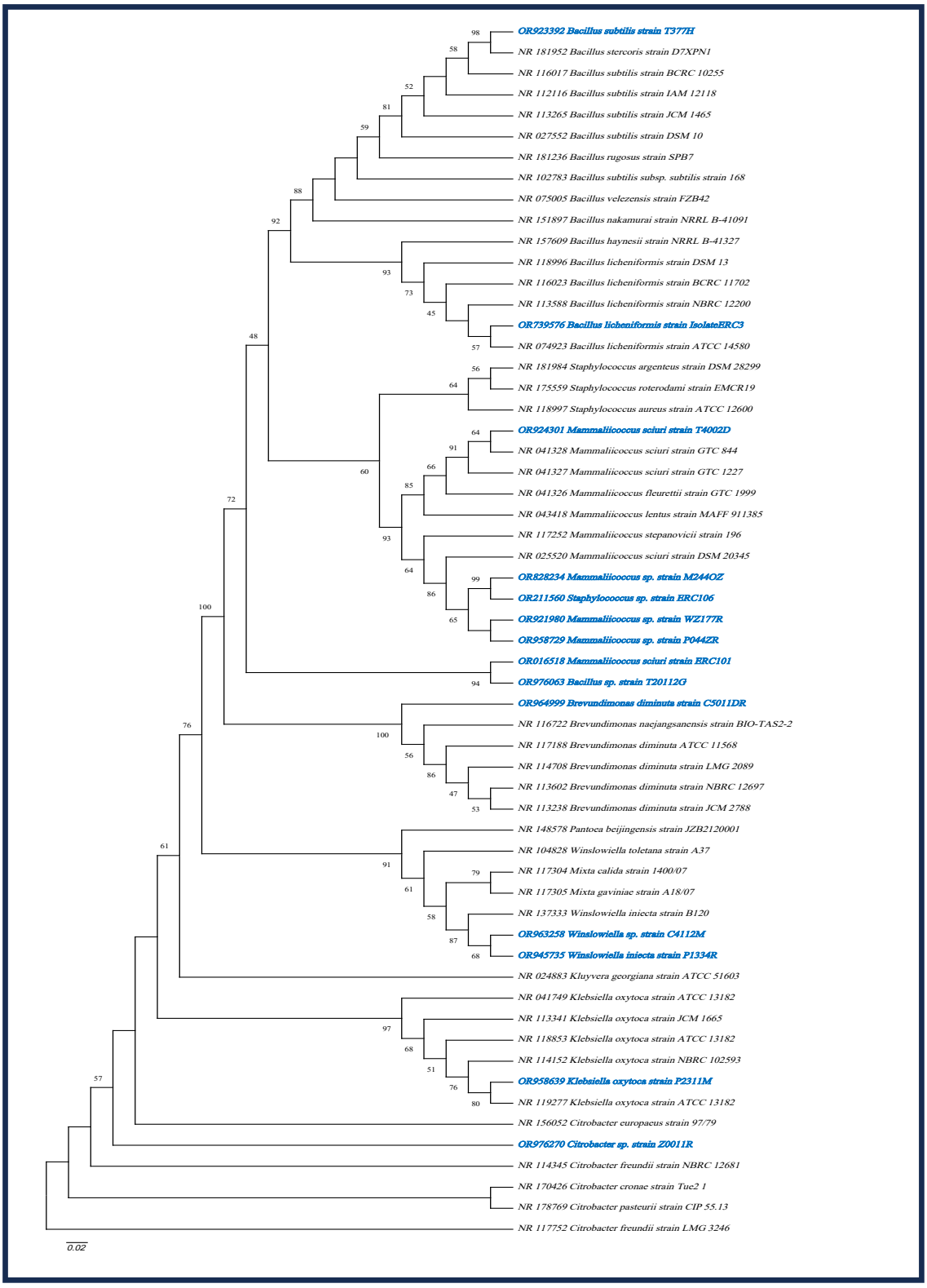

Figure 4.16. Phylogenetic tree of bacterial isolates and closet relatives constructed based on Neighbor-Joining method with bootstrap test of 1000 replicates. The evolutionary distance was calculated based on Maximum Composite Likelihood method.

PLATE: 6

Positive result for qualitative α-amylase and Cellulase activity of bacterial isolates (A to N)

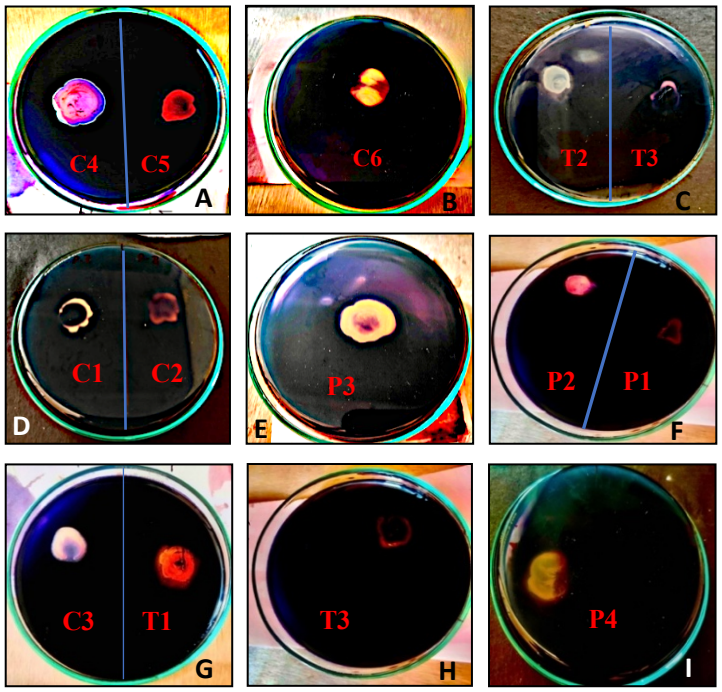

α-amylase positive isolates (A to I): A. Isolate C4 and C5; B. Isolate C6; C. Isolate T2 and T3; D. Isolate P2 and P1; E. Isolate P3; F. Isolate C1and C2; G. Isolate C3 and T1; H. Isolate T3; I. Isolate P4

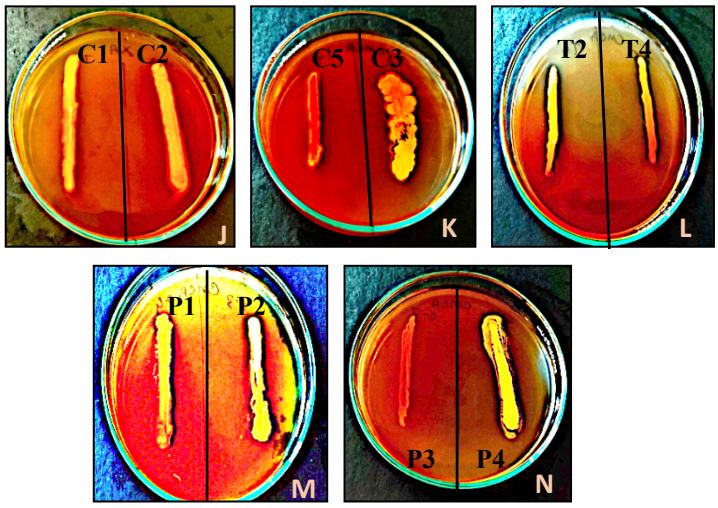

Cellulase positive isolates (J to N): J. Isolate C1 and C2; K. Isolate C5 and C3; L. Isolate T2 and T4; M. Isolate P1 and P2; N. Isolate P3 and P4

PLATE: 7

Positive result for qualitative Proteinase and Lipase activity of bacterial isolates (A to I)

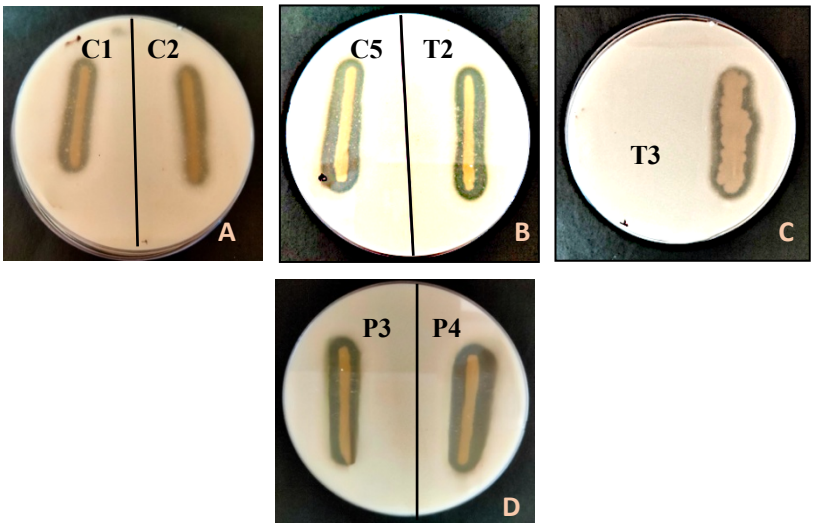

Proteinase positive isolates (A to D): A. Isolate C1 and C2; B. Isolate C5 and T2; C. Isolate T3; D. Isolate P3 and P4

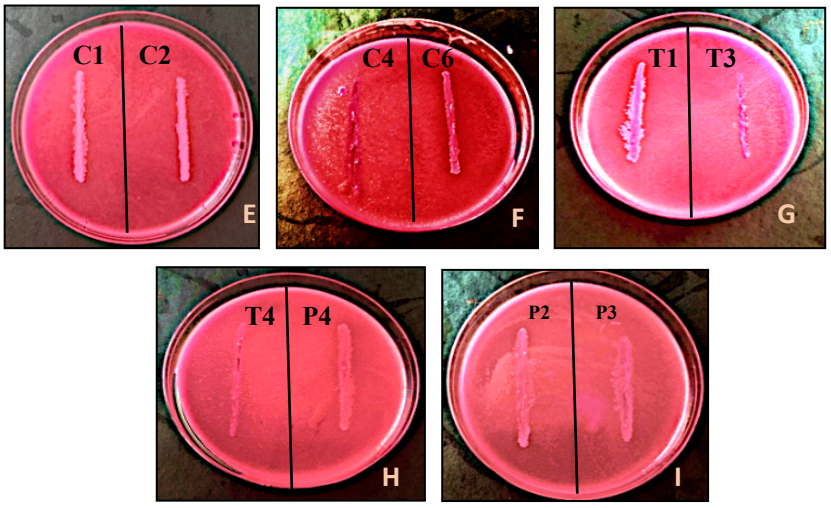

Lipase positive isolates (E to I): E. Isolate C1 and C2; F. isolates C4 and C6; G. Isolate T1 andT3; H. Isolate T4 and P4; I. Isolate P2 and P3

PLATE : 8

Culture plates (A to N): Gut bacterial isolates isolated from *S.ricini* gut reared on *R. communis* (C1-C6); *M. esculenta* (T1-T4); *C. papaya* (P1-P4) leaves

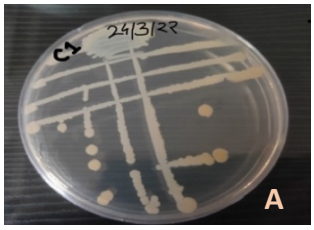

A. Isolate C1

B. Isolate C2

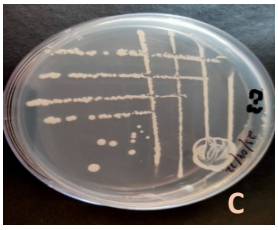

C. Isolate C3

D. Isolate C4

E. Isolate C5

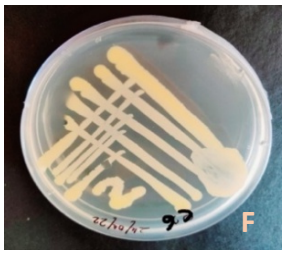

F. Isolate C6

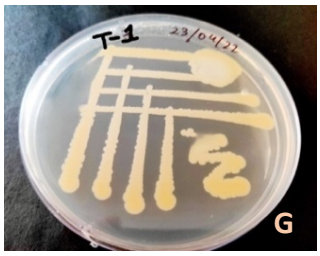

G. Isolate T1

H. Isolate T2

I. Isolate T3

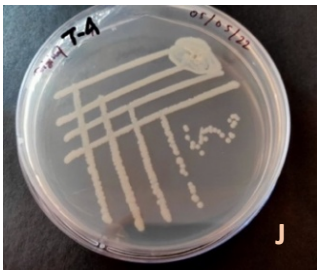

J. Isolate T4

K. Isolate P1

L. Isolate P2

M. Isolate P3

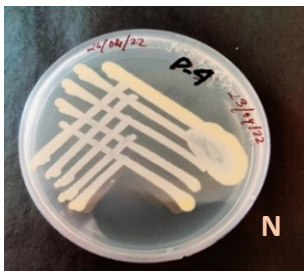

N. Isolate P4

PLATE: 9

Gram staining of gut bacterial Isolates from *S.ricini* gut reared on *R. Communis* (C1-C6); *M.esculenta* (T1-T4); *C. papaya* (P1-P4) leaves

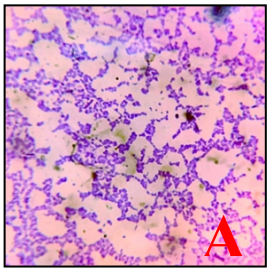

A. Isolate C1

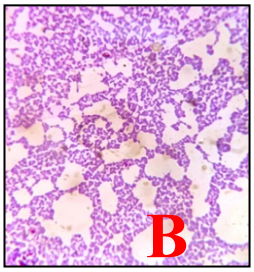

B. Isolate C2

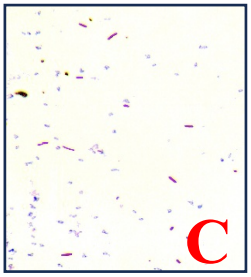

C. Isolate C3

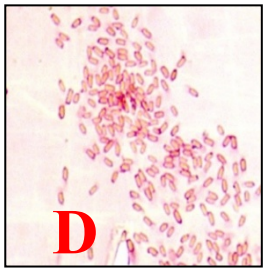

D. Isolate -C4

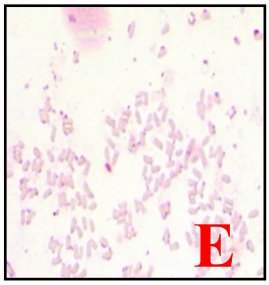

E. Isolate C5

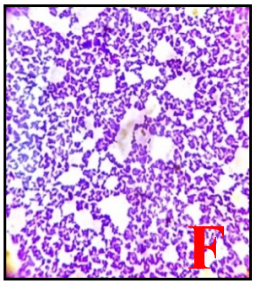

F. Isolate C6

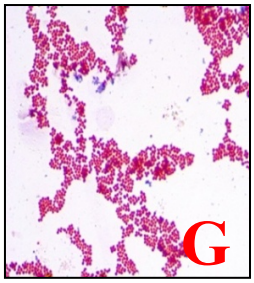

G. Isolate T1

H. Isolate T2

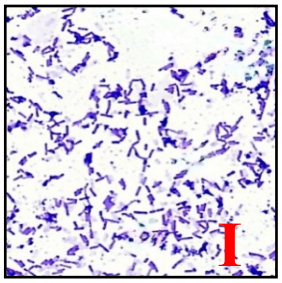

I. Isolate T3

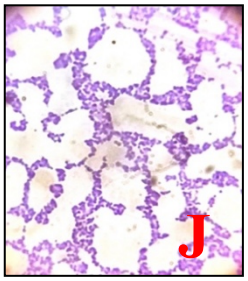

J. Isolate T4

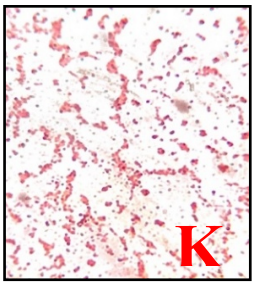

K. Isolate P1

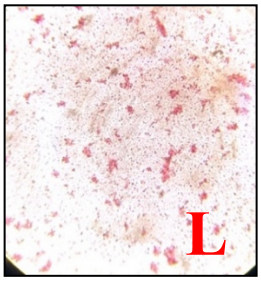

L. Isolate P2

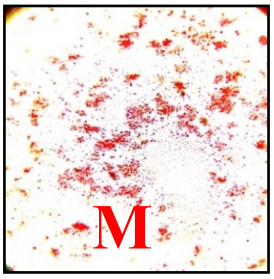

M. Isolate P3

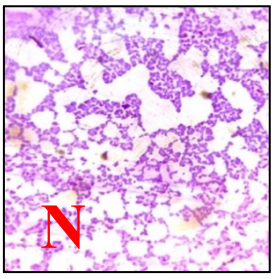

N. Isolate P4